Prior consideration of the referee:

Tsunami modelling is not my field of research, so I think I should not evaluate that part of the work.

Major comments

Comment 1: Given that the innovation of this work with respect Baptista et al. (2006) is that here they propose a geological source for the 1761 earthquake (EQ.), the reader expects to find a strong geological background in this paper supporting their proposal ... and this is not the case. Some important references of the study area should be added to the references list, especially the works focused on the study of tectonic structures mentioned throughout the work (and others missing!). The main problem that I detect in this work is that the proposed geological source for the 1761 EQ does not exist.

Answer 1: We appreciate the referee comments focusing on the geologic background and agree with Sara Martínez-Loriente´s suggestions and added the references accordingly. Also, we completed the present-day geological knowledge of the area and added a geological justification for the choice of the proposed hypothetical fault. To underline our choices, we ameliorated figure 3.

The relationship between seismic and geological sources is quite difficult in the SWIM area, even in the case of instrumental events (for example 28th Feb. 1969). This is a possible consequence of the distributed deformation associated with the slow converging plate boundary. The best contribution to shed light on the characterisation of tsunami (and seismic) hazard in SW Iberian is to use tsunami observations to constrain the location of an active structure. Having said that, the goal of this study is the identification of tectonic features that might justify the tsunami observations of the 31st March 1761; additionally, the source proposed here must be compatible with the area presented by Baptista et al. (2006). Similarly, to the study performed by Baptista et al. (1998) for the 1755 event, here we identify the most likely location and mechanism compatible with the observations. The identification of the geological structure needs extensive marine surveys in the area. However, this is way beyond the scope of our study. The modelling results presented in the manuscript inherit limitations because of the paucity of data and interpretation that it is not always straightforward. However, we were able to present a solution that succeeds in reproducing most of the tsunami observations.

We propose a source location and rupture mechanism compatible with: the results of Baptista et al. (2006) and the set of tsunami travel times and wave heights. We place the candidate source North of the Coral Patch seamount where compressive structures were identified by Hayward et al. (1999) using shallow seismic reflection profiles and side scan sonar data. These structures are also shown in Zitellini et al. (2009).

The text in section 2 now reads:

"The plate boundary between Africa and Eurasia in the NE Atlantic Ocean, the Azores – Gibraltar Fracture Zone (AGFZ), extends from the Azores Triple Junction (ATJ) to the Gibraltar Arc. The main features of the AGFZ are the ATJ; the Gloria Fault (GF) and the SWIM (Fig. 1). At the ATJ, active interplate deformation defines the plate boundary (Fernandes et al., 2006). The GF is a large W-E striking strike-slip fault with scarce seismicity (Laughton and Whitmarsh, 1974) with a strong Mw = 8.3 event on the 25th November 1941 (Gutenberg and Richter, 1949; Moreira, 1984; Baptista et al., 2016). The Gloria fault defines a sharp boundary between Eurasia and Africa (Laughton and Whitmarsh, 1974). Further East, towards the Gulf of Cadiz, in the plate boundary is not clearly defined (Torelli et al., 1997; Zitellini et al., 2009). Large-scale dynamics are imposed by convergence between Africa and Eurasia and by the westward propagation of the Gibraltar Arc. Most recent studies agree that the source of the 1755 Lisbon earthquake with a magnitude of about 8.5±0.3 is in the SWIM (Johnston, 1996; Baptista et al., 1998b; Zitellini et al., 1999; Gutscher et al., 2002; Solares and Arroyo, 2004; Ribeiro et al., 2006).

In the SWIM, two main sets of faults have been identified: Large NE-SW trending thrust faults and WNW-ESE trending dextral strike-slip faults.

Thrust faults include large NE-SW trending structures namely the Horseshoe Fault (HSF) (Gràcia et al., 2003; Zitellini et al., 2004; Terrinha et al., 2009; Martínez-Loriente et al., 2018), the Marquês de Pombal fault (MPF) (Gràcia et al., 2003; Terrinha et al., 2003; Zitellini et al., 2004), the Gorringe bank fault (GBF) (Zitellini et al., 2009; Jiménez-Munt et al., 2010; Sallarès et al., 2013; Martínez-Loriente et al., 2014) and the Coral Patch fault (CPF) (Martínez-Loriente et al., 2013) (Fig. 1). The GBF and the CPF bound the Horseshoe Abyssal Plain (HAP). The NE-SW striking thrusts are deep-rooted faults accompanied by morphological seafloor signatures. Moderate and small magnitude events (M<5) characterise the seismicity of the area. These faults lie between the Gorringe Bank and the Strait of Gibraltar (Custódio et al., 2015). South of the HAP the Coral Patch ridge was identified to have a northern and a southern segment (Martínez-Loriente et al., 2013).

Other smaller NE-SW trending structures are the Sao Vincente Fault (SVF) (Gràcia et al., 2003; Zitellini et al., 2004), the Horseshoe Abyssal Plain Thrust (HAT) (Martínez-Loriente et al., 2014), and to the south of the CPF the Seine Hills (SH) (Martínez-Loriente et al., 2013) (Fig. 1).

The SWIM-Lineaments (LN and LS) (Fig. 1) have been interpreted as the present-day boundary between the Eurasia and Africa plates (Zitellini et al., 2009). They are large WNW-ESE trending dextral strike-slip faults with lengths of ~130 and 180 km for the LN and LS respectively. OBS monitoring captured numerous moderate-magnitude seismic events (Mw 3 – 5) at the intersection of the SWIM faults and NE-SW striking thrusts (Geissler et al., 2010; Silva et al., 2017). Ocean floor morphological signatures like en echelon folds and sets of undulations suggest the quaternary reactivation of the deep-rooted basement faults (Terrinha et al., 2009; Rosas et al., 2009). Terrinha et al. (2009) propose that the present-day deformation in the SWIM is accommodated by strain partitioning of dextral wrenching along the SWIM-Lineaments and thrusting along the NE-SW faults in the Gulf of Cadiz and the HAP. Bartolome et al., (2012) attributes the SWIM faults to have the capacity to trigger Mw > 8.0 earthquakes.

Considering the today known tectonic structures, the CPF is the largescale fault closest located to the source area of the 1761 event suggested by Baptista et al. (2006). This area located southwest of the SWIM faults is in a slow deforming compressive regime driven by the dextral transpressive collision between Africa and Eurasia. Hayward et al. (1999) showed the existence of widespread compressive structures in this region (Coral Patch and Ampere seamounts) based on shallow seismic reflection and side scan sonar data (Fig. 1 and 3). The tectonic deformation uplifted the oceanic crust showing the pervasive original NE-SW striking oceanic fabric formed during oceanic rifting (Hayward et al., 1999; Zitellini et al., 2009). The IGN seismic catalogues list a 6.2 magnitude around the Coral Patch on 11th of July 1915 (Instituto Geográfico Nacional, 2018).

Kinematic plate models (Argus et al., 1989; DeMets et al. 1999; Nocquet and Calais 2004; Fernandes et al., 2007) predict low convergence rates 3 - 5 mm per year between African plates and Eurasia. We used the global kinematic plate model Nuvel-1A. This model is a recalibrated version of the precursor model Nuvel-1 that implements rigid plates and data from plate boundaries such as spreading rates, transform fault azimuths, and earthquake slip vectors (DeMets et al., 1990). The NUVEL 1A model predicts a relatively conservative convergence rate of 3.8 mm per year in the area close to the source area determined by Baptista et al. (2006) for the 1761 tsunami (Fig. 2).

Consequently, we propose a fault extending from the western segment of the CPF towards the epicentre proposed by Baptista et al. (2006). We draw the circle around the Euler pole at -20.61 W, 21.03 N according to the plate kinematic model Nuvel 1-A using Mirone suite (Luis, 2007). To do this, we choose Africa as the fixed plate and Eurasia as the moving plate and draw the circle at the centre of the fault in figure 3. We compute the convergence rate (3.8 mm per year) and plot the tangent velocity vector along the circle (Fig. 3). For this fault, we test different earthquake fault parameters (table 2) and compute the co-seismic deformation using the Mansinha and Smiley equations (Mansinha and Smiley, 1971) implemented in Mirone suite (Luis, 2007). We assume that the initial sea surface elevation mimics the sea bottom deformation and we use it to initiate the tsunami propagation model."

New figure 3 is presented below:

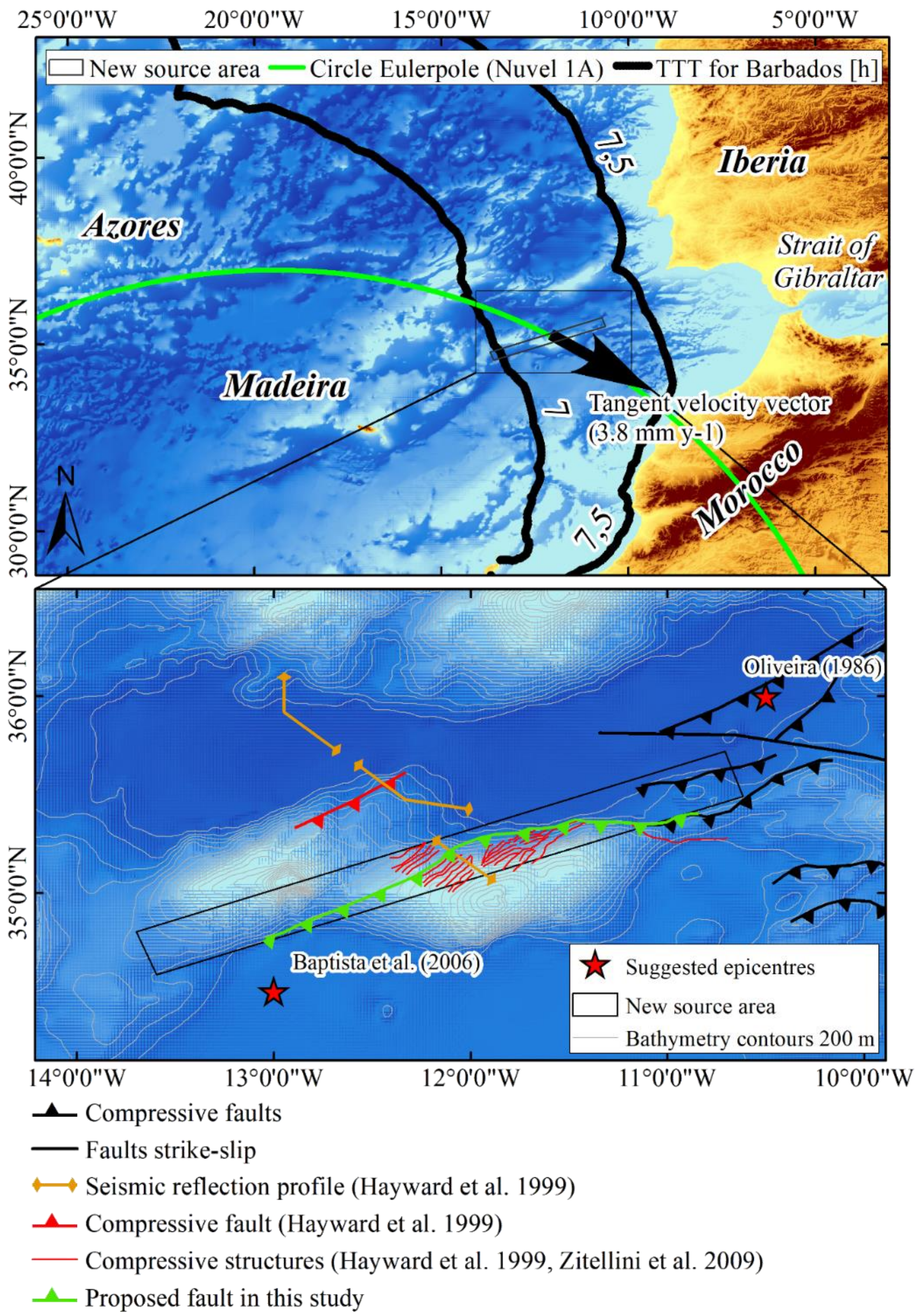

Figure 3. Circle around the Euler pole at the proposed possible source location. The model Nuvel 1A (DeMets et al., 1994, 1999) computes a 3.8 mm y-1 convergence. We plot the tangent velocity vector close to the candidate source. The black lines depict the backward ray tracing contours in hours, for a tsunami travel time (TTT) of 7-7.5 hours to Barbados. In the inset, the black lines plot the thrust and strike-slip faults. The red lines depict the faults and structures proposed in Hayward et al. (1999). The orange lines show the location of the seismic profiles for the areas of the Coral Patch and Ampere seamount (Hayward et al., 1999). The green line identifies the proposed tectonic structure used in this study. The red stars are the locations of the closest proposed epicentres (Baptista et al., 2006 and Oliveira, 1986).

Minor comments

Comment 2:

- Is it really necessary to provide a verbal description of all observations? They appear summarized in tables and figures, and Baptista et al. (2006) can be referenced.

Answer 2: We reduced this section according to the suggestions of referee Uri ten Brink. We believe that the descriptions help the reader to understand the main effects of the tsunami better. However, following Martínez-Loriente suggestion, we shortened the paragraph and kept only the observations that we reassessed.

The manuscript in section 3 now reads:

"Baptista et al. (2006) and Baptista and Miranda (2009) present most of the tsunami observations used herein. Here, we focus on the observations of wave heights, periods, inundation and duration of the sea disturbance that we summarize in table 1. We only reassess the observations in Barbados and Cadiz.

Barbados: Baptista et al. (2006) discarded the arrival time observation in Barbados. However, we find that this is compatible with the source location. The observations report the tsunami arrival at 4 p.m. local time (Mason, 1761; Annual Register, 1761; Borlase, 1762). If we use a solar time difference between Lisbon and Barbados of 3.5 h, as in Baptista et al. (1998a, b), we conclude for a tsunami travel time of 7-7.5h. To validate this TTT, we did a backward ray tracing simulation with a point source in Barbados (see Fig. 2 and 3) and we find that the TTT is compatible with the source area.

Cadiz: The Journal des Matiéres du Temps (Journal Historique, 1773) describes the occurrence of an earthquake in April 1773 and compares it with the 31st March 1761 event. The report concludes that no tsunami was observed in 1773 and suggests a withdraw of the sea after the 31st March 1761 earthquake in the city; however, there are no accounts of inundation neither for the city nor the causeway. We include this observation to constrain the proposed source better.

Table 1 presents a summary of all historical data relevant to the tsunami simulation. Figure 1 shows the locations of the tsunami observations. Wave heights always refer to the maximum positive amplitude above the still water level."

Comment 3: Pag.1, Line 28: The SWIM is not only dominated by NE-SW trending structures. It would be important to mention the WNW-ESE strike-slip SWIM faults and explain a little about them (Rosas et al., 2009; Terrinha et al., 2009; Zitellini et al., 2009; Bartolome et al., 2012; Martínez-Loriente et al., 2013)

Answer 3: We agree with the referee and include the information in our manuscript.

The manuscript in section 1 now reads:

"The coast along the southwest Iberian margin is prone to earthquakes and tsunamis. The earthquake and tsunami catalogues for the Iberian Peninsula and Morocco report three tsunamigenic earthquakes in the 18th century: 1722, 1755 and 1761 (Mezcua and Solares, 1983; Oliveira, 1986; Baptista and Miranda, 2009). While the 1722 event is believed to be a local event (Baptista et al., 2007), the 1st November 1755 and the 31st March 1761 earthquakes generated transatlantic tsunamis (Baptista et al., 1998a, b; Baptista et al., 2003; Baptista et al., 2006; Barkan et al., 2009). The source of the 1755 event has been extensively studied in recent years, e.g. Baptista et al. (1998a, b), Zitellini et al. (2001), Gutscher et al. (2006) and Barkan et al. (2009).

On the contrary, the tectonic source of 31st March 1761 remains poorly understood. The seismic catalogues present different earthquake locations: 10.00 W, 37.00 N (Mezcua and Solares, 1983) or 10.50 W, 36.00 N (Oliveira, 1986). Baptista et al. (2006), used macroseismic intensity data and tsunami travel time observations to locate the source circa 13.00 W, 34.50 N and estimated the magnitude in 8.5. The source location obtained by Baptista et al. (2006) places the 1761 event southwest of the South West Iberian Margin (SWIM) in the outer part of the Gulf of Cadiz (Fig. 1). The plate boundary between Eurasia and Africa is not well defined in the SWIM area as the deformation is distributed over a large area. Here, a complex system of faults accommodates the stress driven by the present-day tectonic regime that is constrained by NW-SE plate convergence between Africa and Eurasia at ~4 mm/yr (Argus et al., 1989; DeMets et al., 1994) and by the westward migration of the Cadiz Subduction slab ~2 mm/yr (Gutscher et al., 2012; Duarte et al., 2013).

The SWIM is dominated by large NE-SW trending structures limiting the Horseshoe Abyssal Plain (HAP). The NE-SW striking structures are the Coral Patch fault (CPF) (Martínez-Loriente et al., 2013), the Gorringe Bank fault (GBF) (Zitellini et al., 2009; Jiménez-Munt et al., 2010; Sallarès et al., 2013; Martínez-Loriente et al., 2014), the Horseshoe fault (HSF) (Gràcia et al., 2003; Zitellini et al., 2004; Martínez-Loriente et al., 2018) and the Marques de Pombal fault (MPF) (Gràcia et al., 2003; Terrinha et al., 2003; Zitellini et al., 2004) (Fig. 1). Other identified NE-SW trending structures are the Sao Vincente Fault (SVF) (Gràcia et al., 2003; Zitellini et al., 2004), the Horseshoe Abyssal Plain Thrust (HAT) (Martínez-Loriente et al., 2014), and to the south of the CPF the Seine Hills (SH) (Martínez-Loriente et al., 2013) (Fig. 1).

Large WNW-ESE trending dextral strike-slip faults (SWIM-Lineaments LN and LS) further characterise the SWIM cutting through the Gulf of Cadiz until the HAP (Zitellini et al., 2009; Terrinha et al., 2009, Rosas et al., 2009) (Fig. 1). To the south, the igneous Ampere and Coral Patch seamounts limit the HAP.

In this study, we investigate the geological source of the 1761 transatlantic tsunami. To do this, we start with a reappraisal of previous research, we analyse the tectonic setting of the area and propose a source compatible with plate kinematics. From this source, we compute the initial sea surface displacement. To propagate the tsunami, we build a bathymetric dataset based on GEBCO (2014) data to compute wave heights offshore the observations points presented in table 1. We also compute inundation using high-resolution digital elevations models comprising topography and bathymetry in Lisbon and Cadiz to compare the results with the observations. Finally, we use Cadiz and Lisbon observations in 1755 and 1761 to compare the size of the events."

We added the following references: (Gràcia et al., 2003; Terrinha et al., 2003; Zitellini et al., 2004; Jiménez-Munt et al., 2010; Sallarès et al., 2013; Martínez-Loriente et al., 2013; Martínez-Loriente et al., 2014; Martínez-Loriente et al., 2018)

Comment 4: Lines 28-30: Please, add the references of the main works carried out in the region focused on each structure. For example: "The SWIM is dominated by large NE-SW trending structures limiting the Horseshoe Abyssal Plain (HAP). The large NE-SW striking structures are the Coral Patch fault (CPF) (Martínez-Loriente et al., 2013), the Gorringe Bank fault (GBF) (Zitellini et al., 2009; Jiménez-Munt et al., 2010; Sallarès et al., 2013; Martínez-Loriente et al., 2014), the Horseshoe fault (HSF) (Gràcia et al., 2003a; Zitellini et al., 2004; Martínez-Loriente et al., 2018) and the Marques de Pombal fault (MPF) (Gràcia et al., 2003a; Terrinha et al., 2003; Zitellini et al., 2004)"; or you can add all the references together at the end (Gràcia et al., 2003a; Terrniha et al., 2003; Zitellini et al., 2004, 2009; Jiménez-Munt et al., 2010; Sallarès et al., 2013; Martínez-Loriente et al., 2013, 2014, 2018, …). Important NE-SW trending structures are missing: the Sao Vicente Fault (SVF) (Gràcia et al., 2003a; Zitellini et al., 2004), the Horseshoe Abyssal Plain Thrust (HAT) (Martínez-Loriente et al., 2014), and the Seine Hills (SH) (Martínez-Loriente et al., 2013).

Answer 4: We agree that the SWIM comprises a certain complexity concerning tectonic structures. We also agree that it is essential to draw a more detailed image of the SWIM and completed with the suggested references.

Please find the changed section of the manuscript in answer #3.

Comment 5: Pag. 2, Figure 1: The figure caption needs to be improved. For example: authors must specify that the red stars refer to source locations; they should explain the difference between green and yellow tsunami observation points; the authors should add other important tectonic structures of the study area such as the SVF, HAT, SH or SWIM faults. The bathymetry used in Figure 1 of Baptista et al. (2016) is much better than the one used in this work to make figures 1, 2, and 3. The authors may consider using the same bathymetry as in the previous work. In addition, the cartography of the Horseshoe and Coral Patch fault traces is very inaccurate, and they appear much longer than they really are. Review the references suggested above to improve them.

Answer 5: We agree with the referee and changed the figures as suggested. The symbols are explained in both the caption and the legend in the figures. The bathymetry we have used in our study is the same used in Baptista et al. (2016). We enhanced the illumination of the maps presented in figures 1,2 and 3. We have also corrected the location and size of the mapped faults.

Please find figure 3 in answer #1. The new figures 1, 2 are presented below:

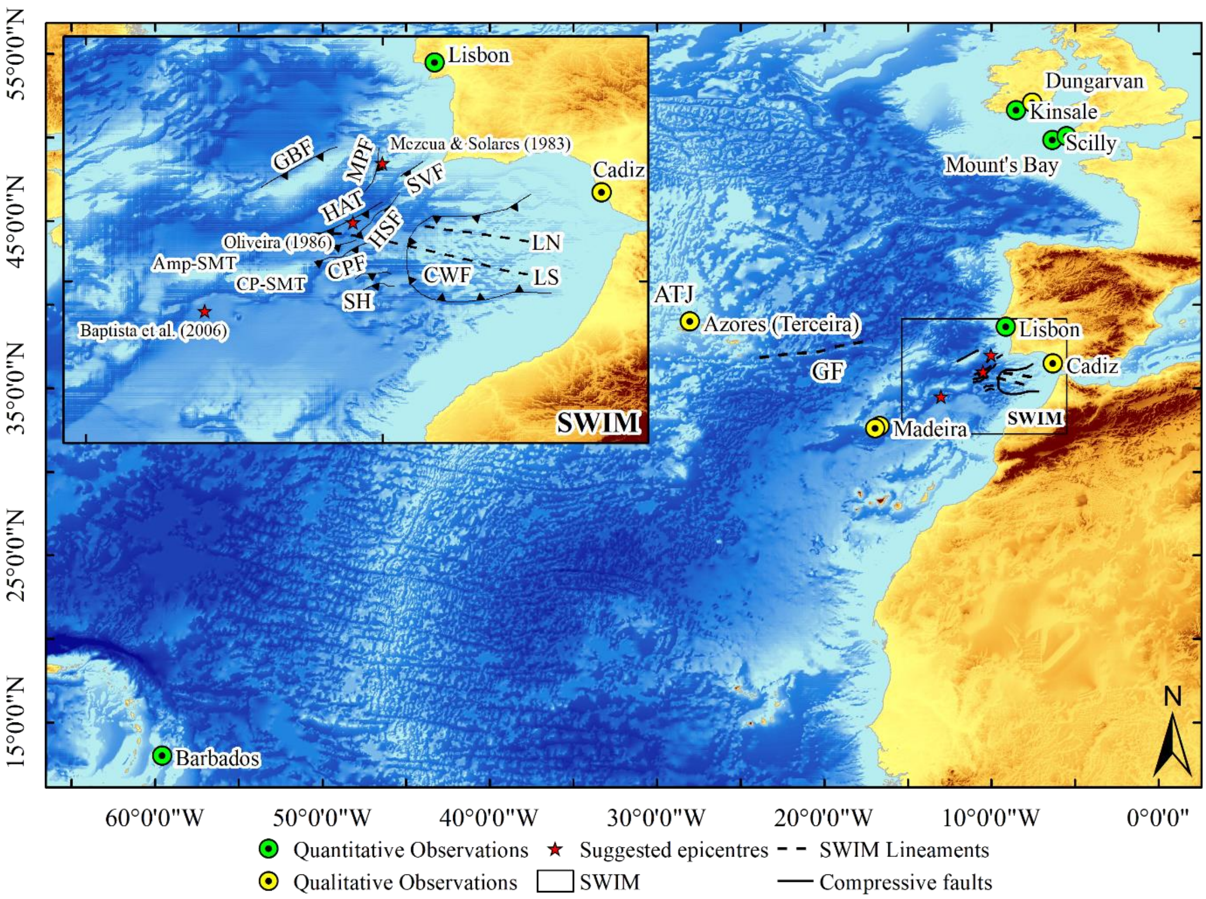

Figure 1. The red stars plot the source location by Oliveira (1986), Mezcua and Solares (1983) and Baptista et al. (2006). The green circles depict the quantitative tsunami observation points, and the yellow circles show the locations of the qualitative descriptions of the tsunami in 1761. The main features of the Azores Gibraltar fracture zone are the Azores Triple Junction (ATJ), the Gloria Fault (GF)

and the Southwest Iberian Margin (SWIM). The inset shows the position of the Ampere seamount (Amp-SMT), the Coral Patch Seamount (CP-SMT) and the locations of the known faults. The black lines mark the faults, and the triangles indicate the direction of dip. The dashed black lines trace the main strike-slip faults. The known thrust faults are the Coral Patch Fault (CPF), the Cadiz Wedge Fault (CWF), the Gorringe Bank fault (GBF), the Horseshoe Fault (HSF) and the Marques de Pombal Fault (MPF). The shown strike-slip faults are the SWIM lineaments (LN) and (LS) and the Gloria Fault (GF).

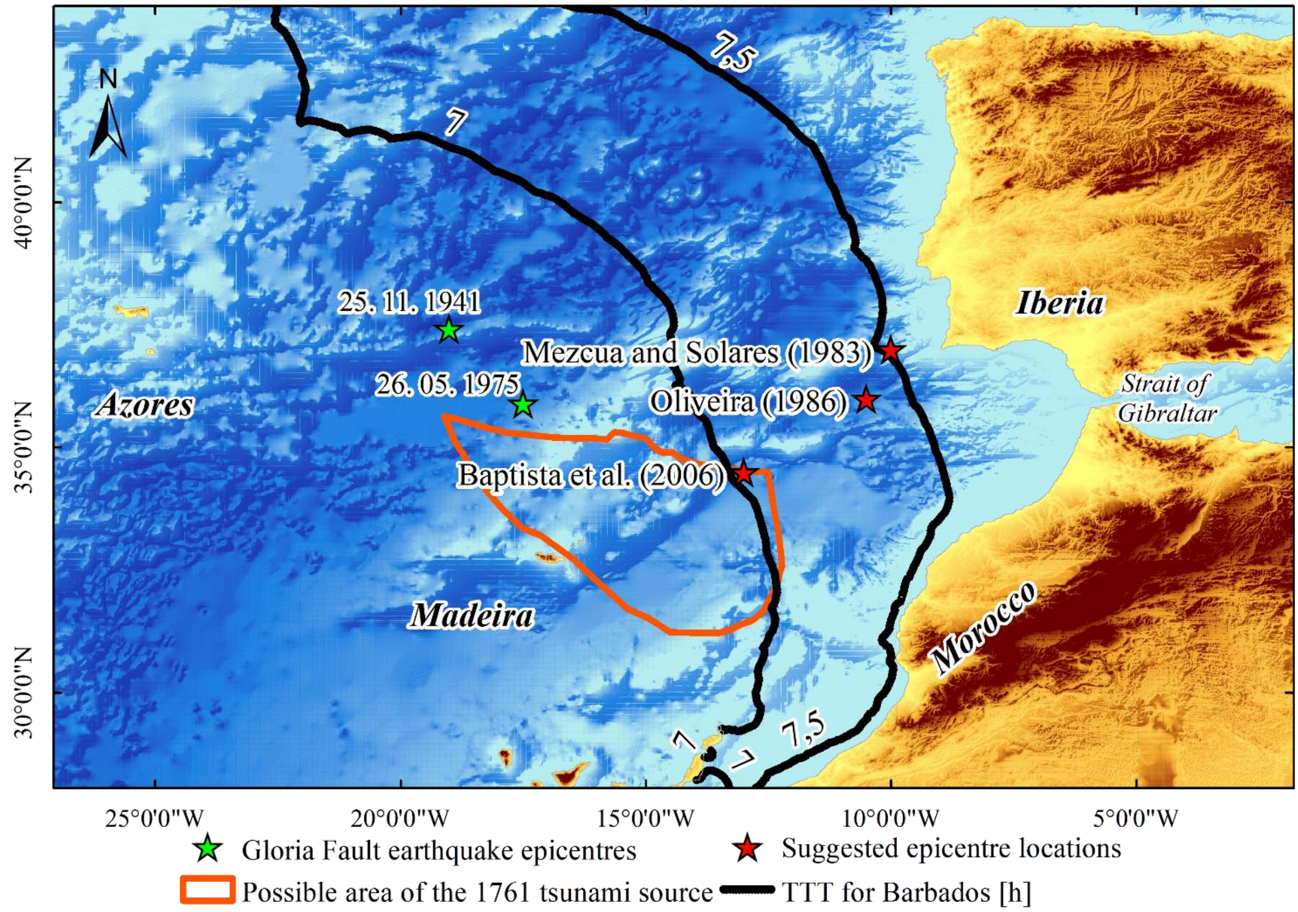

Figure 2. The red stars show the proposed source locations for the 1761 earthquake. The green stars present the epicentres of the two strong magnitude events in the Gloria Fault zone, and the black lines show the backward ray tracing contours for the tsunami travel time (TTT) of 7 – 7.5 hours to Barbados. The limited orange area defines the results obtained using macroseismic analysis combined with backward ray tracing but discarding the TTT for Barbados by Baptista et al. (2006).

Comment 6:

Pag.3
Line 5: To compute inundation a “real” high-resolution bathymetry is needed. The minimum resolution required is 10 m.

Answer 6: Our DEM – digital elevation models, include high-resolution bathymetric data and topographic data. The built of these high-resolution DEMs was possible only for two sites. We specify this in chapter 4.1. We upgraded the bathymetric data with the information presented in the 18th century nautical charts (Bellin, 1762 and Rocque, 1762). These data were interpolated to compute a rectangular grid of 25 m cell size. It is true that accuracy is higher for a DEM with 10 m resolution but if and only if there are measurements to support it, otherwise it is a purely mathematical interpolation.

For our objective to estimate the wave height close to the shore 25 m is a reasonable resolution. Please also see answer #18.

We now better specify in the manuscript.

The manuscript in section 1, paragraph 5 now reads:

"In this study, we investigate the geological source of the 1761 transatlantic tsunami. To do this, we start with a reappraisal of previous research, we analyse the tectonic setting of the area and propose a source compatible with plate kinematics. From this source, we compute the initial sea surface displacement. To propagate the tsunami, we build a bathymetric dataset based on GEBCO (2014) data to compute wave heights offshore the observations points presented in table 1. We also compute inundation using high-resolution digital elevations models comprising topography and bathymetry in Lisbon and Cadiz to compare the results with the observations. Finally, we use Cadiz and Lisbon observations in 1755 and 1761 to compare the size of the events. "

Comment 7: Line 11-12: "with a strong magnitude event on 25th November 1941 …" Specify the magnitude of the seismic event.

Answer 7: We agree and included the magnitude of the event. The manuscript now reads:

The manuscript in section 2, paragraph 1 now reads:

"The GF is a large W-E striking strike-slip fault with scarce seismicity (Laughton and Whitmarsh, 1974) with a strong Mw = 8.3 event on the 25th November 1941 (Gutenberg and Richter, 1949; Moreira, 1984; Baptista et al., 2016)."

Comment 8: Line 18: Same as in Pag.1. Some important NE-SW thrust faults are missing and references should be added.

Answer 8: We agree and added the information.

Please find the changed section 2 in answer #1.

Comment 9: Line 20: "the aseismic SWIM-Lineaments …". Are you sure they are aseismic? Please, review the following references: Geissler et al., 2010, Bartolomé et al., 2012, Grevemeyer et al., 2016, Silva et al., 2017, and references therein.

Answer 9: We agree with the referees' suggestion and changed the manuscript accordingly.

Please find the changed section 2 in answer #1.

Comment 10: Line 23-24: "the Coral Patch ridge (…), with a predominating flower structure geometry". This statement is not true. Review Martínez-Loriente et al., 2013.

Answer 10: We corrected the mistake and rewrote the sentences.

Please find the changed section 2 in answer #1.

Comment 11: Line 25: "the CPF is closest to the area suggest by Baptista et al. (2006)." There is a distance of about 200 km.

Answer 11: This is correct. The hypothetical source we propose is located in between the Coral Patch fault and the epicentre proposed by Baptista et al. (2006). We include in our study the tsunami travel time for Barbados which suggests that the source could be located more to NE. Still of the today known thrust faults the CPF is the structure that is located closest to the area suggested in Baptist et al. (2006). We specified better in the manuscript.

The manuscript in chapter 2, paragraph 6 now reads:

“Considering the today known tectonic structures, the CPF is the largescale fault closest located to the source area of the 1761 event suggested by Baptista et al. (2006). This area located southwest of the SWIM faults is in a slow deforming compressive regime driven by the dextral transpressive collision between Africa and Eurasia. Hayward et al. (1999) showed the existence of widespread compressive structures in this region (Coral Patch and Ampere seamounts) based on shallow seismic reflection and side scan sonar data (Fig. 1 and 3). The tectonic deformation uplifted the oceanic crust showing the pervasive original NE-SW striking oceanic fabric formed during oceanic rifting (Hayward et al., 1999; Zitellini et al., 2009). The IGN seismic catalogues list a 6.2 magnitude around the Coral Patch on 11th of July 1915 (Instituto Geográfico Nacional, 2018).”

Comment 12:

Pag.4
Figure 2: Define “TTT”

Answer 12: TTT was defined in figure 2 and in the manuscript.

Comment 13: Line 7: “we consider a possible fault as an extension of the CPF closest to the area presented by Baptista et al. (2006).” What does this mean? The authors cannot invent faults … Their assumptions have to stick to reality and be based on the structures known in the area.

Answer 13: Please refer to answer #1.

We rephrased the sentences.

The manuscript in section 2, paragraph 8 now reads:

“Consequently, we propose a fault extending from the western segment of the CPF towards the epicentre proposed by Baptista et al. (2006). We draw the circle around the Euler pole at -20.61 W, 21.03 N according to the plate kinematic model Nuvel 1-A using Mirone suite (Luis, 2007). To do this, we choose Africa as the fixed plate and Eurasia as the moving plate and draw the circle at the centre of the fault in figure 3. We compute the convergence rate (3.8 mm per year) and plot the tangent velocity vector along the circle (Fig. 3). For this fault, we test different earthquake fault parameters (table 2) and compute the co-seismic deformation using the Mansinha and Smiley equations (Mansinha and Smiley, 1971) implemented in Mirone suite (Luis, 2007). We assume that the initial sea surface elevation mimics the sea bottom deformation and we use it to initiate the tsunami propagation model.”

Comment 14: Line 11: “we test different earthquake fault parameters (…)” Specify which parameters have been tested

Answer 14: We have included this information in table 2.

Please find the changed manuscript in section 2, paragraph 8.

“For this fault, we test different earthquake fault parameters (table 2) and compute the co-seismic deformation using the Mansinha and Smiley equations (Mansinha and Smiley, 1971) implemented in Mirone suite (Luis, 2007).”

Comment 15: Pag. 6 Line 2: “documents report …” What documents? Add references.

Answers 15: We have changed section 3. The references are presented in table 1.

Please find the changed section 3 in answer #2.

Comment 16: Line 8: Please, provide all measures in international system units.

Answers 16: We rewrote this part. The wave heights of eighteen inches and two feet do not appear anymore in the text. All values used are given in international system units in table 1.

Please find the changed section 3 in answer #2.

Comment 17: Pag. 7 Table 1: All the abbreviations that appear in a figure or Table must be defined in the corresponding figure or table caption. In this case, "TTT".

Answers 17: We have included this information in the table captions.

Comment 18: Pag. 8 Line 8-9: I am in contact with colleagues who are experts in inundation modelling, and they told me that the minimum resolution acceptable to compute inundation is 10 m. Do the authors trust the results obtained with an inadequate bathymetry?

Answers 18: We agree that a higher resolution of bathymetry and topography provides a higher detail of inundation. The bathymetric dataset was updated with local data of nautical charts. Please refer to answer 6.

Comment 19: Pag. 9 Line 2-6: There are like 600 km between the 1941 and 1975 EQ epicentres and the proposed for the 1761 event in Figure 2. I do not understand why the authors have tested the compatibility between these events. It does not make sense to me … In addition, the authors should consider adding the epicentres of these EQ in Figure 2 since they are mentioned in the text.

Answers 19: Other authors (Oliveira 1986; Mezcua and Solares 1983) suggested other epicentres for the 1761 earthquake located to the north to the epicentre concluded by Baptista et al. (2006). Also, the 1975 earthquake epicentre is located close (see figure 2) to the area proposed by Baptista et al. (2006). Both events generated tsunamis we had to consider and discard them as potential sources.

We have included the epicentres of the two events in figure 2. Please see the new figure 2 in answer #5.

Comment 20: Line 21: "(…) the mean dip angle of 40 degrees suggested by Martinez-Loriente et al. (2013)". In the aforementioned reference, a dip of 30° ±5 is suggested for the CPR fault, which is a different structure than the one proposed by the authors as the source of the 1761 EQ. Martinez-Loriente et al., suggest that the CPR does not continue to the west.

Hypothesis A-MS: Based on what geological knowledge of the area do the authors propose this solution? Do the authors know any structure in the area that is subdivided into 4 segments each of 50 km long?

Answers 20: We rewrote this section in our manuscript. We propose hypothesis A-MS on basis of the modelling solutions that reproduce the tsunami observations at the time. Please find our comment on the chosen scenarios in answer #1.

The manuscript in sub-section 4.2, paragraph 4 now reads:

"Hypotheses A and A-MS: Here we use a strike angle compatible with the study by Martínez-Loriente et al., (2013) that follows the morphology of the Coral Patch scarp and seamount (Fig. 1 and Fig. 3). To take into account the tectonic regime of the source area we choose fault plane parameters compatible with a structure of compressive nature. The velocity vector predicted by NUVEL 1A (Fig. 3) together with the short tsunami wave periods (4-12 minutes) reported in 1761 (table 1) are in line with the chosen dip angle of 40 degrees (table 2). On the other hand, Martínez-Loriente et al. (2013) suggest for the Coral Patch Faults dip angles of 30±5 degrees dip and a rake angle of 90 degrees. These authors also conclude that the fault root is between 7 and 13 km depth. We approximate the rake angle according to the difference between the convergence arrow given by the circle around the Euler Pole and the fault plane (Fig. 3)."

Comment 21: Pag 10 Table 2: What is the rationale for using these values? For example, the depth for "Hyp. A" is 10 km … On the basis of what information do the authors choose this value? or a width of 50 km (????)

Answers 21: The depth of the fault root is suggested in Martinez-Loriente et al. (2013) between about 7 - 8 and 12 - 13 kilometers depth. We have chosen the width to be compatible with the scaling laws of Wells and Coppersmith (1994), Manighetti et al. (2007), Blaser et al. (2010) and Matias et al. (2013). All other values are specified in the manuscript.

Please find the changed manuscript in answer #20.

Comment 22: Hypothesis B: I do not know any strike-slip fault with NE-SW orientation and 280 km long (!!!) at the proposed source location for the 1761 EQ.

We use hypothesis B to check if a fault with predominant strike-slip mechanism may reproduce the tsunami observations.

Please find our answer regarding the hypothetical scenarios in answer #1.

Comment 23: Pag 18 Line 27: "It is possible to find a geological source compatible with the source area deduced from TTTs and with macro-seismic intensity data" Really? What is the "real" geological source proposed by the authors? In Figure 3, the proposed fault plane does not correspond to any real geological structure.

Answers 23: We agree with the referee that this statement may be too strong in the sense that we did not do a marine survey to look for this structure. We rephrased the sentences. Figure 3 shows the location of the candidate source, and we clearly state in section 4 that we consider Hypotheses A, A-MS and B.

Please find our answer regarding the proposed hypothetical sources in answer #1.

The revised manuscript in section 6 and 7, now reads:

"Considering the points discussed above, we conclude our preferred solution is A-MS. Following facts justify our choice:

• The candidate source in hypothesis A-MS is compatible with the geodynamic setting predicted by the NUVEL 1A model (DeMets et al., 1999). NE/SW compressive structures with comparable fault plane parameters have been identified close to the Coral Patch seamount (Fig. 1 and 3). The proposed structure is possibly propagating and reactivating the NE-SW striking oceanic rifting fabric towards the epicentre suggested by Baptista et al. (2006). Nevertheless, we must stress that Martínez-Loriente et al. (2013) do not suggest an extension of the seismogenic structure at the CPF although no detailed multi-channel seismic survey has been carried out to the west of the CPF in the proposed source area.

• The wave heights produced by the numerical models are in better agreement with proposed source A-MS.

• Wave heights greater than 14 m produced by hypothesis B would result in a catastrophic scenario which is rather unlikely and nor observed neither or reported. Also, 4.2 m wave height produced by hypothesis B in the Azores would have caused inundation, which has not been reported.

• Although both solutions follow our considerations for Lisbon, the wave heights generated by source A-MS seem to be more comparable to the observed fluctuation of 2.4 m than the wave heights produced by source B.

• The larger drawdown in Cadiz favours solution A-MS.

The reassessment of the reports of Barbados and Cadiz support the choice selected here. While the tsunami travel time for Barbados supports the source location, the fact that there was no inundation reports in Cadiz supports the magnitude and rupture mechanism proposed here.

7. Conclusion

• The source proposed here for the 1761 event is compatible with the tsunami observation dataset, the macro-seismic intensity data (Baptista et al., 2006) and with the geodynamic context of the area predicted by the kinematic plate model NUVEL 1-A.

• The source proposed here is located in the SWIM, an area of widespread compressive structures (Hayward et al., 1999), corresponding to a fault that extends from the western segment of the CPF towards the epicentre proposed by Baptista et al. (2006).

The investigation of each historical event in the area contributes to a better understanding of the structure of this diffuse plate boundary and ultimately leads to a better evaluation of the seismic and tsunami hazard. This study together with the study by Baptista et al. (2006) underlines the need to include the 1761 event in all seismic and tsunami hazard assessments in the Northeast Atlantic basin."

The following references listed below are now included in the manuscript:

Bartolome, R., Gràcia, E., Stich, D., Martínez-Loriente, S., Klaeschen, D., de Lis Mancilla, F., Lo Iacono, C., Dañobeitia, J. J. and Zitellini, N.: Evidence for active strike-slip faulting along the Eurasia-Africa convergence zone: Implications for seismic hazard in the southwest Iberian margin. Geology, 40(6), 495-498, 2012.

Geissler, W. H., Matias, L., Stich, D., Carrilho, F., Jokat, W., Monna, S., IbenBrahim, A. Mancilla, F., Gutscher, M.-A., Sallarès, V., Zitellini, N.: Focal mechanisms for sub–crustal earthquakes in the Gulf of Cadiz from a dense OBS deployment. Geophysical Research Letters 37, L18309, doi:10.1029/2010GL044289, 2010.

Gràcia, E., Dañobeitia, J.J., Vergés, J. and PARSIFAL Team: Mapping active faults offshore Portugal (36N– 38N): Implications for seismic hazard assessment along the southwest Iberian margin. Geology, 31(1), 83–86, 2003.

Hayward, A., Watts, A. B., Westbrook G. K., Collier J. S.: A seismic reflection and GLORIA study of compressional deformation in the Gorringe Bank region, Eastern North Atlantic. Geophysical Journal International 138, 831–850, doi:10.1046/j.1365-246x.1999.00912.x, 1999.

Jiménez-Munt, I., Fernàndez, M., Vergés, J., Afonso, J.C., Garcia-Castellanos, D., Fullea, J.: Lithospheric structure of the Gorringe Bank: Insights into its origin and tectonic evolution. Tectonics 29. doi:10.1029/2009TC002458, 2010.

Martínez-Loriente, S., Sallarès, V., Gràcia, E., Bartolome, R., Dañobeitia, J. J., Zitellini, N.: Seismic and gravity constraints on the nature of the basement in the Africa-Eurasia plate boundary: New insights for the geodynamic evolution of the SW Iberian Margin. Journal of Geophysical Research 119, 127-149, doi:10.1002/2013JB010476, 2014.

Martínez-Loriente, S., Gràcia, E., Bartolome, R., Perea, H., Klaeschen, D., Dañobeitia, J. J., Zitellini, N., Wynn, R. B. and Masson, D. G.: Morphostructure, tectono-sedimentary evolution and seismic potential of the Horseshoe Fault, SW Iberian Margin. Basin Res, 30: 382-400. doi:10.1111/bre.12225, 2018.

Matias, L. M., Cunha, T., Annunziato, A., Baptista, M. A., and Carrilho, F. (2013). Tsunamigenic earthquakes in the Gulf of Cadiz: fault model and recurrence. Natural hazards and earth system sciences, 13(1), 1-13.

Sallarès, V., Martínez-Loriente, S., Prada, M., Gràcia, E., Ranero, C. R., Gutscher, M. A., Bartolome, R., Gailler, A., Dañobeitia, J. J., Zitellini, N.: Seismic evidence of exhumed mantle rock basement at the Gorringe Bank and the adjacent Horseshoe and Tagus abyssal plains (SW Iberia). Earth and Planetary Science Letters 365, 120–131, doi:10.1016/j.epsl.2013.01.021, 2013.

Silva, S., Terrinha, P., Matias, L., Duarte, J. C., Roque, C., Ranero, C. R., Geissler, W., H. and Zitellini, N.: Micro-seismicity in the Gulf of Cadiz: Is there a link between micro-seismicity, high magnitude earthquakes and active faults?. Tectonophysics, 717, 226-241, 2017.

Terrinha, P., Pinheiro, L. M., Henriet, J. P., Matias, L., Ivanov, M. K., Monteiro, J. H., Akhmetzhanov, A., Volkonskaya, A., Cunha, T., Shaskin, P., and Rovere, M.: Tsunamigenic-seismogenic structures, neotectonics, sedimentary processes and slope instability on the southwest Portuguese Margin. Marine Geology, 195(1-4), 55-73, 2003.

Terrinha, P. , Matias, L., Vicente, J., Duarte, J., Luís, J., Pinheiro, L., Lourenço, N., Diez, S. Rosas, F., Magalhães, V., Valadares, V., Zitellini, N., Roque, C., Mendes Víctor, L. and MATESPRO Team.: Morphotectonics and strain partitioning at the Iberia–Africa plate boundary from multibeam and seismic reflection data, Marine Geology, 267, 3-4, 156-174, https://doi.org/10.1016/j.margeo.2009.09.012, 2009.

Torelli, L., Sartori, R., Zitellini, N.: The giant chaotic body in the Atlantic Ocean off Gibraltar: new results from a deep seismic reflection survey. Marine and Petroleum Geology 14 (2), 125–134, doi:10.1016/S0264-8172(96)00060-8, 1997.

Zitellini, N., Rovere, M., Terrinha, P., Chierici, F., Matias, L. and BIGSETS Team: Neogene through Quaternary tectonic reactivation of SW Iberian Passive Margin. Pure Applied Geophysics, 161, 565–587, 2004.

Zitellini, N., Gràcia, E., Matias, L., Terrinha, P., Abreu, M. A. DeAlteriis, G., Henriet, J.P., Dañobeitia, J.J., Masson, D.G., Mulder, T., Ramella, R., Somoza, L., and Diez, S.: The quest for the Africa–Eurasia plate boundary west of the Strait of Gibraltar, Earth and Planetary Science Letters, 280, 1-4, 13-50, https://doi.org/10.1016/j.epsl.2008.12.005, 2009.

Reanalysis of the 1761 transatlantic tsunami

Martin Wronna[1,3], Maria Ana Baptista[1,2], Jorge Miguel Miranda[1,3]

1 Instituto Dom Luiz, Faculdade de Ciências da Universidade de Lisboa, Portugal
2 Instituto Superior de Engenharia de Lisboa, Instituto Politécnico de Lisboa, Portugal
3 Instituto Português do Mar e da Atmosfera, IP, Lisboa, Portugal

Correspondence to: Martin Wronna (Mawronna@fc.ul.pt)

Abstract. The segment of the Africa-Eurasia plate boundary between the Gloria fault and the Strait of Gibraltar has been the set of significant tsunamigenic earthquakes. However, their precise location and rupture mechanism remains poorly understood. The investigation of each event contributes to a better understanding of the structure of this diffuse plate boundary and ultimately leads to a better evaluation of the seismic and tsunami hazard. The 31st March 1761 event is one of the few known transatlantic tsunamis. Macroseismic data and tsunami travel times were used in previous studies to assess its source area. However, no one discussed the geological source of this event. In this study, we present a reappraisal of tsunami data to show that the observations dataset is compatible with a geological source close to Coral Patch and Ampere seamounts. We constrain the rupture mechanism with plate kinematics and the tectonic setting of the area. This study favours the hypothesis that the 1761 event occurred in the southwest of the likely location of the 1st November 1755 in a slow deforming compressive regime driven by the dextral transpressive collision between Africa and Eurasia.

1. Introduction

The coast along the southwest Iberian margin is prone to earthquakes and tsunamis. The earthquake and tsunami catalogues for the Iberian Peninsula and Morocco report three tsunamigenic earthquakes in the 18th century: 1722, 1755 and 1761 (Mezcua and Solares, 1983; Oliveira, 1986; Baptista and Miranda, 2009). While the 1722 event is believed to be a local event (Baptista et al., 2007), the 1st November 1755 and the 31st March 1761 earthquakes generated transatlantic tsunamis (Baptista et al., 1998a, b; Baptista et al., 2003; Baptista et al., 2006; Barkan et al., 2009). The source of the 1755 event has been extensively studied in recent years, e.g. Baptista et al. (1998a, b), Zitellini et al. (2001), Gutscher et al. (2006) and Barkan et al. (2009).

On the contrary, the tectonic source of 31[st] March 1761 remains poorly understood. The seismic catalogues present different earthquake locations: 10.00 W, 37.00 N (Mezcua and Solares, 1983) or 10.50 W, 36.00 N (Oliveira, 1986). Baptista et al. (2006), used macroseismic intensity data and tsunami travel time observations to locate the source circa 13.00 W, 34.50 N and estimated the magnitude in 8.5. The source location obtained by Baptista et al. (2006) places the 1761 event southwest of the South West Iberian Margin (SWIM) in the outer part of the Gulf of Cadiz (Fig. 1).

Formatted: English (United Kingdom)
Formatted: English (United Kingdom)
Formatted: English (United Kingdom)
Formatted: English (United Kingdom)
Formatted: English (United Kingdom)
Formatted: English (United Kingdom)

The plate boundary between Eurasia and Africa is not well defined in the SWIM area as the deformation is distributed over a large area. Here, a complex system of faults accommodates the stress driven by the~~The~~ present-~~-~~day tectonic regime that is constrained by NW-SE plate convergence between Africa and Eurasia at ~4 mm/yr (Argus et al., 1989; DeMets et al., 1994) and by the westward migration of the Cadiz Subduction slab ~2 mm/yr (Gutscher et al., 2012; Duarte et al., 2013).

The SWIM is dominated by large NE-SW trending structures limiting the Horseshoe Abyssal Plain (HAP). The ~~large~~ NE-SW striking structures are the Coral Patch fault (CPF) (Martínez-Loriente et al., 2013), the Gorringe Bank fault (GBF) (Zitellini et al., 2009; Jiménez-Munt et al., 2010; Sallarès et al., 2013; Martínez-Loriente et al., 2014), the Horseshoe fault (HSF) (Gràcia et al., 2003; Zitellini et al., 2004; Martínez-Loriente et al., 2018) and the Marques de Pombal fault (MPF) (Gràcia et al., 2003; Terrinha et al., 2003; Zitellini et al., 2004) (Fig. 1). Other identified NE-SW trending structures are the Sao Vincente Fault (SVF) (Gràcia et al., 2003; Zitellini et al., 2004), the Horseshoe Abyssal Plain Thrust (HAT) (Martínez-Loriente et al., 2014), and to the south of the CPF the Seine Hills (SH) (Martínez-Loriente et al., 2013) (Fig. 1).

Large WNW-ESE trending dextral strike-slip faults (SWIM-Lineaments LN and LS) further characterise the SWIM cutting through the Gulf of Cadiz until the HAP (Zitellini et al., 2009; Terrinha et al., 2009, Rosas et al., 2009) (Fig. 1). To the south, ~~the HAP is limited by~~ the igneous Ampere and Coral Patch seamounts limit the HAP. ~~The present-day tectonic regime is constrained by NW-SE plate convergence between Africa and Eurasia at ~4 mm/yr (Argus et al., 1989; DeMets et al., 1994) and westward migration of the Cadiz Subduction slab ~2 mm/yr (Gutscher et al., 2012; Duarte et al., 2013).~~

~~Figure 1. Source location by Baptista et al. (2006) and the tsunami observation points of the tsunami in 1761. The main features of the Azores Gibraltar fracture zone are the Azores Triple Junction (ATJ), the Gloria Fault (GF) and the Southwest Iberian Margin (SWIM). The inset shows the position of the Ampere seamount (Amp-SMT), the Coral Patch Seamount (CP-SMT) and the locations of the known faults. The black lines mark the faults, and the triangles indicate the direction of dip. The known faults are the Coral Patch Fault (CPF), the Cadiz Wedge Fault (CWF), the Gorringe Bank fault (GBF), the Horseshoe Fault (HSF) and the Marques de Pombal Fault (MPF).~~

Formatted: English (United Kingdom)

Formatted: English (United Kingdom)

Formatted: English (United Kingdom)

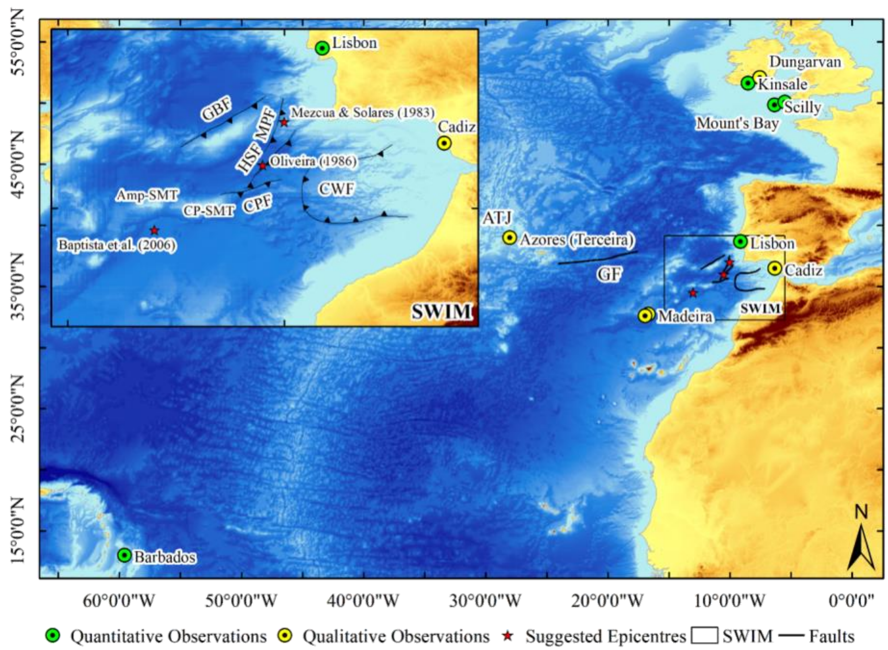

55°0'0"N
45°0'0"N
35°0'0"N
25°0'0"N
15°0'0"N
60°0'0"W
50°0'0"W
40°0'0"W
30°0'0"W
20°0'0"W
10°0'0"W
0°0'0"
Lisbon
Cadiz
GBF
MPF
HSF
Mezcua & Solares (1983)
Oliveira (1986)
CWF
Amp-SMT
CP-SMT
CPF
Baptista et al. (2006)
SWIM
Dungarvan
Kinsale
Scilly
Mount's Bay
ATJ
Azores (Terceira)
GF
Madeira
Barbados
N
Quantitative Observations
Qualitative Observations
Suggested Epicentres
SWIM
Faults

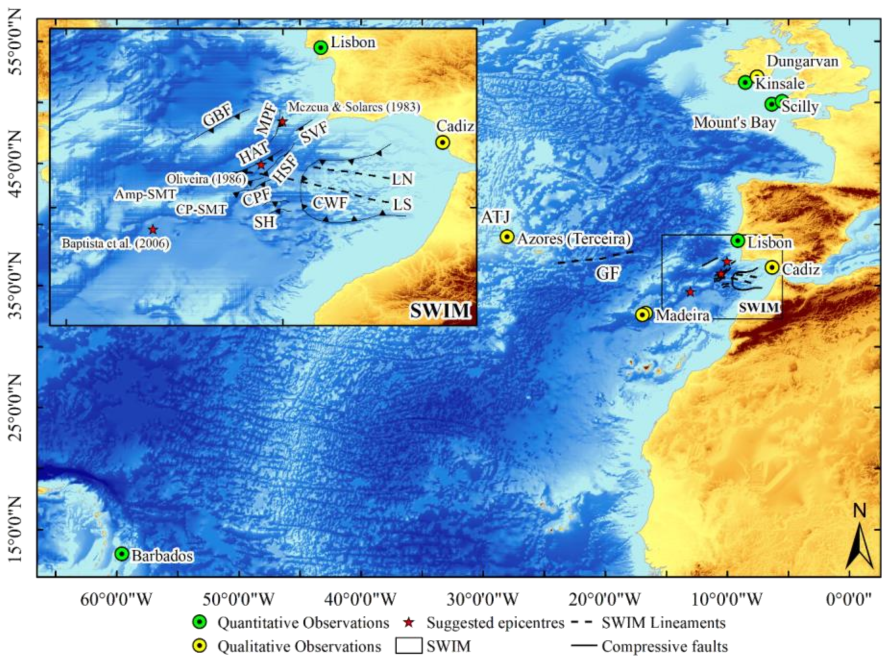

Formatted: English (United Kingdom)

Figure 1. The red stars plot the ~~S~~source location by ~~Baptista et al. (2006)~~Oliveira (1986), Mezcua and Solares (1983) and~~-~~ Baptista et al. (2006). ~~and the~~The green circles depict the quantitative tsunami observation points, and the yellow circles show the locations of the qualitative descriptions of the tsunami in 1761. The main features of the Azores Gibraltar fracture zone are the Azores Triple Junction (ATJ), the Gloria Fault (GF) and the Southwest Iberian Margin (SWIM). The inset shows the position of the Ampere seamount (Amp-SMT), the Coral Patch Seamount (CP-SMT) and the locations of the known faults. The black lines mark the faults, and the triangles indicate the direction of dip. The dashed black lines trace the main strike-slip faults. The known thrust faults are the Coral Patch Fault (CPF), the Cadiz Wedge Fault (CWF), the Gorringe Bank fault (GBF), the Horseshoe Fault (HSF) and the Marques de Pombal Fault (MPF). The shown strike-slip faults are the SWIM lineaments (LN) and (LS) and the Gloria Fault (GF).

Formatted: English (United Kingdom)

In this study, we investigate the geological source of the 1761 transatlantic tsunami. To do this, we start with a reappraisal of previous research, we analy~~s~~ze the tectonic setting of the area and propose a source compatible with plate kinematics. From this source, we compute the initial sea surface displacement. To propagate the tsunami, we build a bathymetric dataset based on GEBCO (2014) data to compute wave heights offshore the observations points presented in table 1. We also compute inundation using high~~-~~resolution digital elevations models comprising topography and bathymetry in Lisbon and Cadiz to compare the results with the observations. Finally, we use Cadiz and Lisbon observations in 1755 and 1761 to compare the size of the events.

Formatted: English (United Kingdom)

Formatted: English (United Kingdom)

Formatted: English (United Kingdom)

2. Geodynamical context

The plate boundary between Africa and Eurasia in the NE Atlantic Ocean, the Azores – Gibraltar Fracture Zone (AGFZ), extends from the Azores Triple Junction (ATJ) to the Gibraltar Arc. The main features of the AGFZ are the ATJ; the Gloria Fault (GF) and the SWIM (Fig. 1). At the ATJ, active interplate deformation defines the plate boundary (Fernandes et al., 2006). The GF is a large W-E striking strike-slip fault with scarce seismicity (Laughton and Whitmarsh, 1974) with a strong Mw = 8.3 event on the 25th November 1941 (Gutenberg and Richter, 1949; Moreira, 1984; Baptista et al., 2016). The Gloria fault defines a sharp boundary between Eurasia and Africa (Laughton and Whitmarsh, 1974). Further East, towards the Gulf of Cadiz, in the plate boundary is not clearly defined (Torelli et al., 1997; Zitellini et al., 2009). Large-scale dynamics are imposed by convergence between Africa and Eurasia and by the westward propagation of the Gibraltar Arc. Most recent studies agree that the source of the 1755 Lisbon earthquake with a magnitude of about 8.5±0.3 is in the SWIM (Johnston, 1996; Baptista et al., 1998b; Zitellini et al., 1999; Gutscher et al., 2002; Solares and Arroyo, 2004; Ribeiro et al., 2006).

In the SWIM, two main sets of faults have been identified: Large NE-SW trending thrust faults and WNW-ESE trending dextral strike-slip faults.

Thrust faults include large NE-SW trending structures namely the Horseshoe Fault (HSF) (Gràcia et al., 2003; Zitellini et al., 2004; Terrinha et al., 2009; Martínez-Loriente et al., 2018), the Marquês de Pombal fault (MPF) (Gràcia et al., 2003; Terrinha et al., 2003; Zitellini et al., 2004), the Gorringe bank fault (GBF) (Zitellini et al., 2009; Jiménez-Munt et al., 2010; Sallarès et al., 2013; Martínez-Loriente et al., 2014) and the Coral Patch fault (CPF) (Martínez-Loriente et al., 2013) (Fig. 1). The GBF and the CPF bound the Horseshoe Abyssal Plain (HAP). The NE-SW striking thrusts are deep-rooted faults accompanied by morphological seafloor signatures. Moderate and small magnitude events (M<5) characterise the seismicity of the area. These faults lie between the Gorringe Bank and the Strait of Gibraltar (Custódio et al., 2015). South of the HAP the Coral Patch ridge was identified to have a northern and a southern segment (Martínez-Loriente et al., 2013).

Other smaller NE-SW trending structures are the Sao Vincente Fault (SVF) (Gràcia et al., 2003; Zitellini et al., 2004), the Horseshoe Abyssal Plain Thrust (HAT) (Martínez-Loriente et al., 2014), and to the south of the CPF the Seine Hills (SH) (Martínez-Loriente et al., 2013) (Fig. 1).

The SWIM-Lineaments (LN and LS) (Fig. 1) have been interpreted as the present-day boundary between the Eurasia and Africa plates (Zitellini et al., 2009). They are large WNW-ESE trending dextral strike-slip faults with lengths of ~130 and 180 km for the LN and LS respectively. OBS monitoring captured numerous moderate-magnitude seismic events (Mw 3 – 5) at the intersection of the SWIM faults and NE-SW striking thrusts (Geissler et al., 2010; Silva et al., 2017). Ocean floor morphological signatures like en echelon folds and sets of undulations suggest the quaternary reactivation of the deep-rooted basement faults (Terrinha et al., 2009; Rosas et al., 2009). Terrinha et al. (2009) propose that the present-day deformation in the SWIM is accommodated by strain partitioning of dextral wrenching along the SWIM-Lineaments and thrusting along the NE-SW faults in the Gulf of Cadiz and the HAP. Bartolome et al., (2012) attributes the SWIM faults to have the capacity to trigger Mw > 8.0 earthquakes.

Formatted: English (United Kingdom)

Formatted: English (United Kingdom)

Formatted: English (United Kingdom)

Formatted: English (United Kingdom)

Formatted: English (United Kingdom)

Formatted: English (United Kingdom)

Considering the today known tectonic structures, the CPF is the largescale fault closest located to the source area of the 1761 event suggested by Baptista et al. (2006). This area located southwest of the SWIM faults is in a slow deforming compressive regime driven by the dextral transpressive collision between Africa and Eurasia. Hayward et al. (1999) showed the existence of widespread compressive structures in this region (Coral Patch and Ampere seamounts) based on shallow seismic reflection and side scan sonar data (Fig. 1 and 3). The tectonic deformation uplifted the oceanic crust showing the pervasive original NE-SW striking oceanic fabric formed during oceanic rifting (Hayward et al., 1999; Zitellini et al., 2009). The IGN seismic catalogues list a 6.2 magnitude around the Coral Patch on 11th of July 1915 (Instituto Geográfico Nacional, 2018).

Formatted: English (United Kingdom)

Kinematic plate models (Argus et al., 1989; DeMets et al. 1999; Nocquet and Calais 2004; Fernandes et al., 2007) predict low convergence rates 3 - 5 mm per year between African plates and Eurasia. We used the global kinematic plate model Nuvel-1A. This model is a recalibrated version of the precursor model Nuvel-1 that implements rigid plates and data from plate boundaries such as spreading rates, transform fault azimuths, and earthquake slip vectors (DeMets et al., 1990). The NUVEL 1A model predicts a relatively conservative convergence rate of 3.8 mm per year in the area close to the source area determined by Baptista et al. (2006) for the 1761 tsunami (Fig. 2).

The western segment of the plate boundary between Africa and Eurasia in the NE Atlantic Ocean extends from the Azores Triple Junction (ATJ) to Gibraltar. The main features of the Azores Gibraltar fracture zone are the ATJ; the Gloria Fault (GF) and the SWIM (Fig. 1). At the ATJ, the plate boundary is defined by active interplate deformation (Fernandes et al., 2006). The GF is a large W-E striking transverse fault with scarce seismicity (Laughton and Whitmarsh, 1974) with a strong magnitude event on 25th November 1941 (Gutenberg and Richter, 1949; Moreira, 1984; Baptista et al., 2016). The Gloria fault defines a sharp boundary between Eurasia and Africa (Laughton and Whitmarsh, 1974). Further East, towards the Gulf of Cadiz, in the SWIM area the plate boundary is not clearly defined (Zitellini et al., 2009). Large scale dynamics are imposed by convergence between Africa and Eurasia and by the westward propagation of the Gibraltar arc. Most recent studies agree that the source of the 1755 Lisbon earthquake with a magnitude of about 8.5±0.3 is in the SWIM (Johnston, 1996; Baptista et al., 1998; Zitellini et al., 1999; Gutscher et al., 2002; Solares and Arroyo, 2004; Ribeiro et al., 2006). Identified faults in the SWIM include large NE-SW trending thrust faults namely the Horseshoe Fault (HSF), the Marquês de Pombal fault (MPF), the Gorringe bank fault (GBF) and the Coral Patch fault (CPF) (Fig. 1). The GBF and the CPF bound the Horseshoe Abyssal Plain (HAP) The NE-SW striking thrusts are deep rooted faults accompanied with morphological seafloor signatures. Moderate and small magnitude events (M<5) characterize the seismicity of the area.These faults lie between the Gorringe Bank and the Strait of Gibraltar (Custódio et al., 2015). South of the HAP the Coral Patch ridge shows surface deformation, with a predominating flower structure geometry (Rosas et al., 2009; Terrinha et al., 2009; Martínez-Loriente et al., 2013).and the aseismic SWIM-Lineaments – WNW-ESE trending dextral strike-slip faults (Zitellini et al., 2009). The NE-SW striking thrusts are deep rooted faults accompanied with morphological seafloor signatures. Moderate and small magnitude events (M<5) characterize the seismicity of the area. These faults lie between the Gorringe Bank and the Strait of Gibraltar (Custódio et al., 2015). South of the HAP the Coral Patch ridge shows surface deformation, with a predominating flower structure geometry (Rosas et al., 2009; Terrinha et al., 2009; Martínez-Loriente et al., 2013).

Considering the earlier mentioned faults, the CPF is closest to the area suggest by Baptista et al. (2006). Also, this area southwest of the SWIM, is in a slow deforming compressive regime dictated by the major tectonic driving forces (Eurasia – Africa convergence and Gibraltar arc westward propagation). The IGN seismic catalogs list a 6.2 magnitude around the Coral Patch on 11th of July 1915.

Kinematic plate models (Argus et al., 1989; DeMets et al. 1999; Nocquet and Calais 2004; Fernandes et al., 2007) predict low convergence rates 3 - 5 mm per year between African plates and Eurasia. We used the global kinematic plate model Nuvel-1A. This model is a recalibrated version of the precursor model Nuvel-1 that implements rigid plates and data from plate boundaries such as spreading rates, transform fault azimuths, and earthquake slip vectors (DeMets et al., 1990). The NUVEL 1A model predicts a relatively conservative convergence rate of 3.8 mm per year in the area close to the source area determined by Baptista et al. (2006) for the 1761 tsunami (Fig. 2).

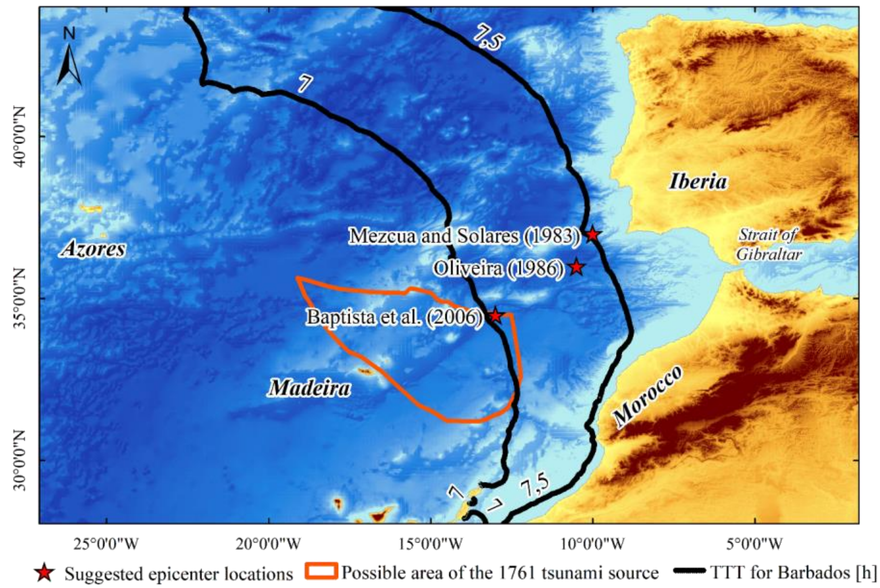
N
7.5
7
Iberia
Mezcua and Solares (1983)
Oliveira (1986)
Baptista et al. (2006)
Azores
Strait of Gibraltar
Madeira
Morocco
7
7
7.5
40°0'0"N
35°0'0"N
30°0'0"N
25°0'0"W
20°0'0"W
15°0'0"W
10°0'0"W
5°0'0"W
Suggested epicenter locations
Possible area of the 1761 tsunami source
TTT for Barbados [h]

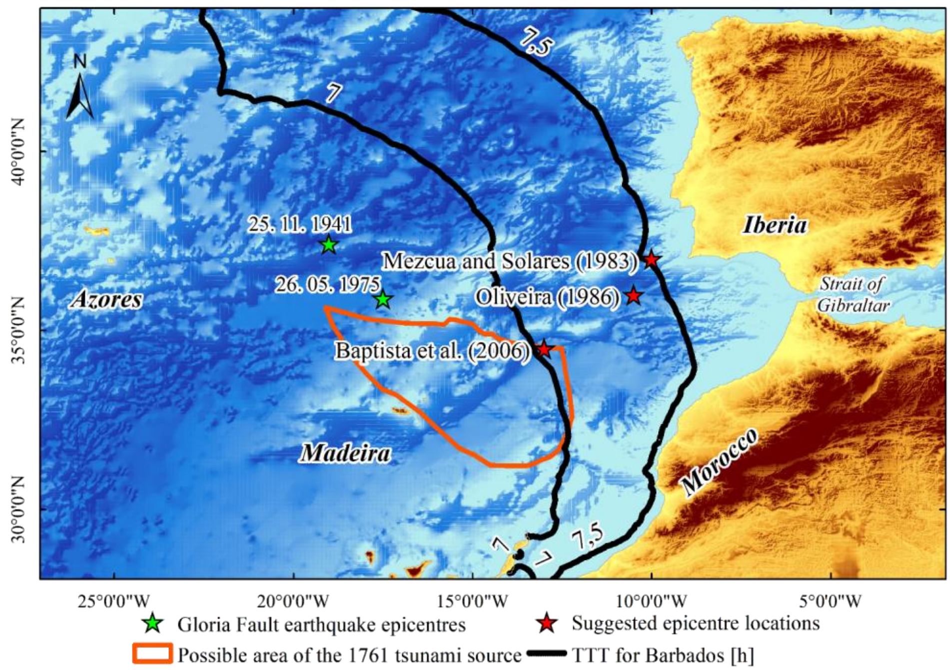

Figure 2. The red stars show the proposed sSource locations for the 1761 earthquake. The green stars present the epicentres of the two strong magnitude events in the Gloria Fault zone, and the black lines show the backward ray tracing contours (black lines) for the tsunami travel time (TTT) of 7 – 7.5 hours to Barbados. The limited orange limited area defines the results obtained using macroseismic analysis combined with backward ray tracing but discarding the TTT for Barbados by Baptista et al. (2006).

Consequently, we propose a fault extending from the western segment of the CPF towards the epicentre proposed by Baptista et al. (2006)Consequently, we consider a possible fault as an extension of the CPF closest .to the area presented by Baptista et al. (2006) .-We draw the circle around the Euler pole at -20.61 Ww, 21.03 N according to the plate kinematic model Nuvel 1-A using Mirone suite (Luis, 2007). To do this, we choose Africa as the fixed plate and Eurasia as the moving plate and draw the circle at the centreer of the fault in figure 3. We compute the convergence rate (3.8 mm per year) and plot the tangent velocity vector along the circle (Fig. 3). For this fault, we test different earthquake fault parameters (table 2) and compute the co-seismic deformation using the Mansinha and Smiley equations (Mansinha and Smiley, 1971) implemented in Mirone suite (Luis, 2007). We assume that the initial sea surface elevation mimics the sea bottom deformation and we use it to initiate the tsunami propagation model.

Formatted: English (United Kingdom)

Formatted: English (United Kingdom)
Formatted: English (United Kingdom)
Formatted: English (United Kingdom)
Formatted: English (United Kingdom)
Formatted: English (United Kingdom)
Formatted: English (United Kingdom)
Formatted: English (United Kingdom)
Formatted: English (United Kingdom)

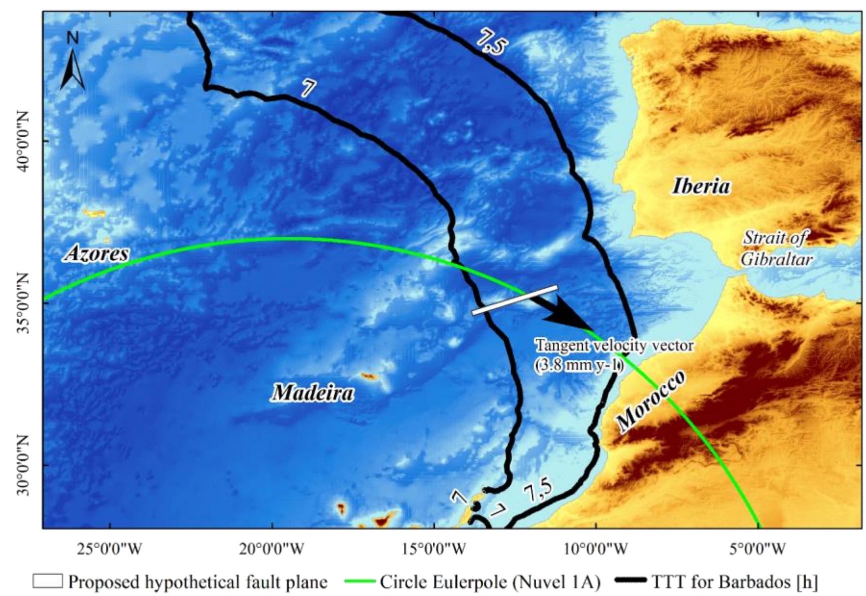
N
7,5
7
40°0'0"N
Iberia
Strait of
Gibraltar
Azores
35°0'0"N
Tangent velocity vector
(3.8 mm y-1)
Madeira
Morocco
30°0'0"N
7
7
7,5
25°0'0"W
20°0'0"W
15°0'0"W
10°0'0"W
5°0'0"W
Proposed hypothetical fault plane
Circle Eulerpole (Nuvel 1A)
TTT for Barbados [h]

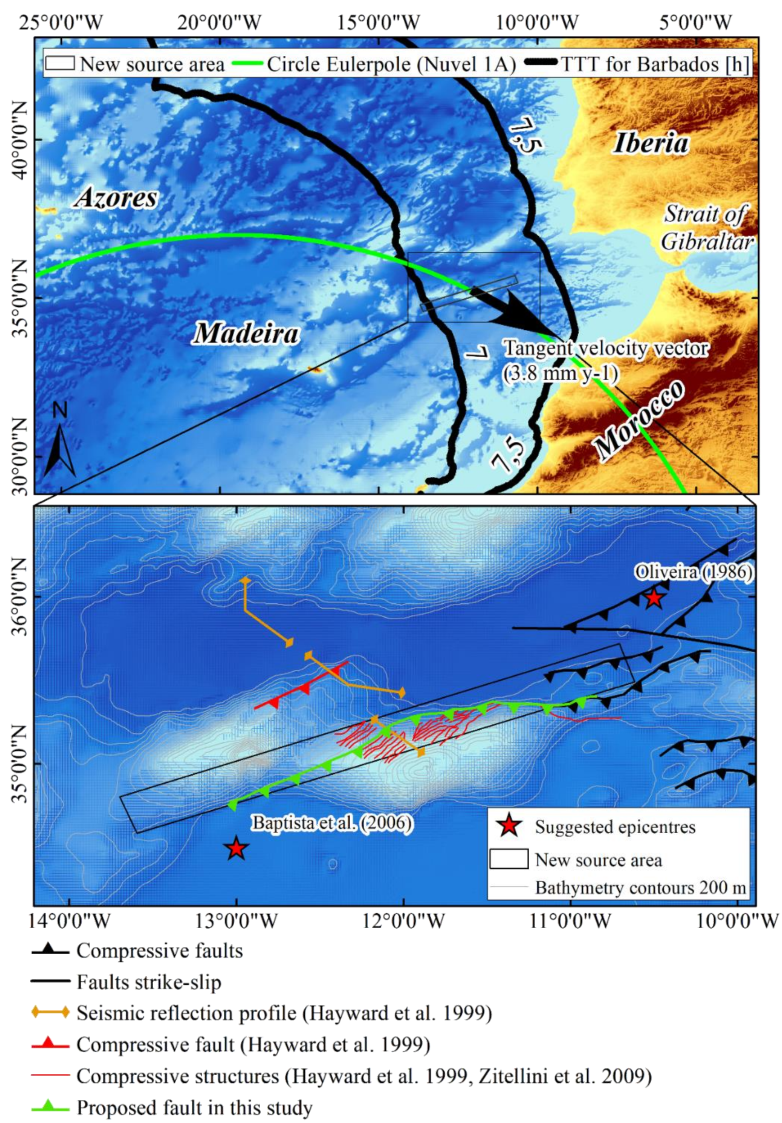

Formatted: English (United Kingdom)

Figure 3. Circle around the Euler pole at the proposed possible source location. The model Nuvel 1A (DeMets et al., 1994, 1999) computes a 3.8 mm y-1 convergence. We plot the tangent velocity vector close to the candidate source. The black lines depict the backward ray tracing contours in hours, for a tsunami travel time (TTT) of 7-7.5 hours to Barbados. In the inset, the black lines plot the thrust and strike-slip faults. The red lines depict the faults and structures proposed in Hayward et al. (1999). The orange lines show the location of the seismic profiles for the areas of the Coral Patch and Ampere seamount (Hayward et al., 1999). The green line identifies the proposed tectonic structure used in this study. The red stars are the locations of the closest proposed epicentres (Baptista et al., 2006 and Oliveira, 1986).Figure 3. Circle around the Euler pole at the proposed hypothetical fault location. The model Nuvel 1A (DeMets et al., 1994, 1999) computes a 3.8 mm y^{-1} convergence. We plot the tangent velocity vector at the proposed fault. The black lines depict the backward ray tracing contours in hours, for TTT of 7-7.5 hours to Barbados.

3. Reassessment of historical data on the 1761 tsunami

Baptista et al. (2006) and Baptista and Miranda (2009) present most of the tsunami observations used herein. Here, we focus on the observations of wave heights, periods, inundation and duration of the sea disturbance that we summarise in table 1. We only reassess the observations in Barbados and Cadiz.

Barbados: Baptista et al. (2006) discarded the arrival time observation in Barbados. However, we find that this is compatible with the source location. The observations report the tsunami arrival at 4 p.m. local time (Mason, 1761; Annual Register, 1761; Borlase, 1762). If we use a solar time difference between Lisbon and Barbados of 3.5 h, as in Baptista et al. (1998a, b), we conclude for a tsunami travel time of 7-7.5h. To validate this TTT, we did a backward ray tracing simulation with a point source in Barbados (see Fig. 2 and 3) and we find that the TTT is compatible with the source area.

Cadiz: The Journal des Matiéres du Temps (Journal Historique, 1773) describes the occurrence of an earthquake in April 1773 and compares it with the 31st March 1761 event. The report concludes that no tsunami was observed in 1773 and suggests a withdraw of the sea after the 31st March 1761 earthquake in the city; however, there are no accounts of inundation neither for the city nor the causeway. We include this observation to constrain the proposed source better.The studies by Baptista et al. (2006) and Baptista and Miranda (2009) present most of the tsunami information used herein. However, only the information on tsunami travel times was used by these authors to locate the source (Baptista et al., 2006).

In this study, we reappraise the tsunami observations regarding tsunami travel time and wave heights, period and duration of the sea disturbance.

For Cadiz, the Journal des Matiéres du Temps (Journal Historique, 1773), describes the occurrence of an earthquake in April 1773 and compares it with the 31st March 1761 event. The document states that in April 1773, following an earthquake felt in Cadiz, it was feared that it could have triggered a tsunami. The governor of the city ordered the closing of the town gates to prevent people fleeing to the causeway which was inundated in 1755. The report concludes that no tsunami was observed in 1773. However, the text of the report suggests a withdraw of the sea after the 31st March 1761 earthquake in the city.

We assume as in Baptista et al. (1998a, b) that all times are solar time and we re-evaluate the Tsunami Travel Time (TTT) for Barbados. Here, documents report a tsunami arrival at a 4 pm local time. Baptista et al. (2006) concluded for the unreliability of this observation and did not use it in the backward ray tracing simulations to locate the source. In this study, we use 3.5 hours solar time difference between Lisbon and Barbados. Using 4 pm local time as stated in Borlase (1762) for the arrival of the tsunami and the 3.5 h solar time difference between Lisbon and Barbados, we conclude that the TTT shoub be between 7-

Formatted: English (United Kingdom)
Formatted: English (United Kingdom)
Formatted: English (United Kingdom)
Formatted: Font color: Auto, English (United Kingdom)
Formatted: Font color: Auto, English (United Kingdom)
Formatted: Font color: Auto, English (United Kingdom)
Formatted: Font color: Auto, English (United Kingdom)
Formatted: Font color: Auto, English (United Kingdom)
Formatted: English (United Kingdom)
Formatted: Font color: Auto, English (United Kingdom)
Formatted: Font color: Auto, English (United Kingdom)
Formatted: English (United Kingdom)
Formatted: Font color: Auto, English (United Kingdom)
Formatted: English (United Kingdom)
Formatted: Font color: Auto, English (United Kingdom)
Formatted: English (United Kingdom)
Formatted: Font color: Auto, English (United Kingdom)
Formatted: English (United Kingdom)
Formatted: Font color: Auto, English (United Kingdom)
Formatted: English (United Kingdom)
Formatted: Font color: Auto, English (United Kingdom)
Formatted: English (United Kingdom)
Formatted: Font color: Auto, English (United Kingdom)
Formatted: Font color: Auto, English (United Kingdom)
Formatted: English (United Kingdom)

~~7.5 h. We place a point source at Barbados and use backward ray tracing and find that the 7 h contour falls within the area presented by Baptista et al. (2006) close to their suggested location (Fig. 1 and 2) at 34.50 N 13.00 W. Mason (1761) wrote that the tide ebbed and flowed between eighteen inches and two feet in Barbados.~~

~~The reports contain many observations about the abnormal motion of the sea. For Lisbon, the reports state abnormal motion of the sea about 1 hour and 15 minutes after the earthquakes. Two sources (Unknown, 1761 and Molloy, 1761) describe a flowing and ebbing of 8 feet of about six minutes while Borlase (1762) reports only three to four feet. All three reports agree that the agitation lasted until the evening.~~

~~The descriptions from northern Europe include Mount's Bay, Scilly Islands, Kinsale and Dungarvan (Table 1 and Figure 1).~~

~~Borlase (1762) reports the tsunami observations at several points in Mount's Bay. The waves arrived around five o'clock in the afternoon at about one and a half hour before full ebb. According to the report, the water rose between four and six feet, and the sea advanced and recessed five times within an hour (Table 1).~~

~~At Scilly Islands, the report states that the sea rose four feet and that the agitation lasted about 2 hours. In Kinsale, the Annual Register (1761) states that at 6 p.m. at low water, the tide rose quickly about two feet higher than it was and it ebbed again about four minutes later. The movement of the fluxes repeated several times but with decreasing intensity after the in and out flux. In Dungarvan, Borlase (1762) states that the sea ebbed and flowed five times between 4 and 9 o'clock in the afternoon.~~

Table 1 presents a summary of all historical data relevant to the tsunami simulation. Figure 1 shows the locations of the tsunami observations. Wave heights always refer to the maximum positive amplitude above the still water level.

Table 1. Summary of the available data of the 1761 tsunami at the time. The column TTT lists the observed Tsunami Travel Times. The column polarity indicates the first movement of the sea upward (U) or downward (D).

Location	Lon. [°]	Lat. [°]	Local Time	TTT [h]	Wave height [m]	Polarity	Period [min]	Duration	Source
Lisbon	-9.13	38.72º	13:15	1.25	1.2 - 1.8	-	6	Lasted until night	Unknown (1761); Molloy (1761); Borlase (1762)
Cadiz	-6.29	36.52	-	-	-	D	-	-	Journal des Matieres du Temps (1773)
Kinsale	-8.51	51.67	18:00	6	0.6	U	4	Repeated several times	Annual Register (1761); Borlase (1762)
Scilly Islands	-6.38	49.92	17:00	5	0.6 - 1.2	U	-	> 2 hours	Borlase (1762)
Mount's Bay	-5.48	50.08	17:00	5	1.2 - 1.8	U	12	1 hour	Borlase (1762)
Dungarvan	-7.48	51.95	16:00	4	-	-	-	5 hours	Borlase (1762)
Barbados	-59.57	13.03	16:00	7 - 8	0.45 - 0.6	-	8	4 hours but lasted until 6 in the morning.	Mason (1761); Annual Register (1761)
	-59.57	13.03			0.6	-	3 - 6	Increased again at ten for short time then decreased.	Borlase (1762)
Madeira	-16.91	32.62	-	-	~1; higher in the East	-	-	Lasted longer in the East than in the South.	Heberden (1761)
Azores	-27.22	38.65	-	-	Large	U	Some min.	3 hours	Fearns (1761)

Formatted: English (United Kingdom)
Formatted: English (United Kingdom)
Formatted: English (United Kingdom)
Formatted: English (United Kingdom)
Formatted: Font: (Default) +Body (Times New Roman), English (United Kingdom)
Formatted Table
Formatted: Font: (Default) +Body (Times New Roman), English (United Kingdom)
Formatted: Left
Formatted: Font: (Default) +Body (Times New Roman)
Formatted: Font: (Default) +Body (Times New Roman), English (United Kingdom)
Formatted: Left
Formatted: Font: (Default) +Body (Times New Roman), English (United Kingdom)
Formatted: Left
Formatted: Font: (Default) +Body (Times New Roman), English (United Kingdom)
Formatted: Left
Formatted: Font: (Default) +Body (Times New Roman), English (United Kingdom)
Formatted: Left
Formatted: Font: (Default) +Body (Times New Roman), English (United Kingdom)
Formatted: Left
Formatted: Left
Formatted: Font: (Default) +Body (Times New Roman), English (United Kingdom)
Formatted: Left
Formatted: Font: (Default) +Body (Times New Roman), English (United Kingdom)
Formatted Table
Formatted: Left
Formatted: Font: (Default) +Body (Times New Roman), English (United Kingdom)
Formatted: Left
Formatted: English (United Kingdom)

4. Tsunami Simulations

4.1 The numerical model

We used the code NSWING (Non-linear Shallow Water model wIth Nested Grids) for numerical tsunami modelling. The code solves linear and non-linear shallow water equations (SWEs) in a Cartesian or spherical reference frame using a system of nested grids and a moving boundary condition to track the shoreline motion based on COMCOT (Cornell Multi-grid Coupled Tsunami Model; Liu et al., 1995; 1998). The code was benchmarked with the analytical tests presented by Synolakis et al. (2008) and tested in Miranda et al. (2014) and Baptista et al. (~~2016~~2016), Wronna et al. (2015) and Omira et al. (2015).

For Cadiz and Lisbon only, where high-resolution bathymetric data was available, we employed a set of coupled nested grids with a final resolution of 25 m to compute inundation. We compute a new bathymetric dataset using the nautical charts close to the coast or LIDAR data to build a Digital Terrain Model to compute inundation in Lisbon and Cadiz. Close to the tsunami source we interpolate bathymetry data (GEBCO, 2014) to obtain a 1600 m grid cell size. We apply a refinement factor of 4 for the four nested grids. Consequently, the intermediate grids have a resolution of 100 m and 400 m respectively. In Cadiz, we use the soundings and coastline of historical nautical charts from the 18th century (Bellin, 1762 and Rocque, 1762) to compute a Paleo Digital Elevation Model (PDEM) (Wronna et al., 2017). To do this, we geo-referenced the old nautical charts and use the modern-day DEM (UG-ICN, 2009) to implement the information from the ancient charts. According to Wronna et al. (2017), we systematically remodelled bathymetry and the coastline.

To initiate the tsunami propagation model, we compute the co-seismic deformation according to the half-space elastic theory (Mansinha and Smylie, 1971) implemented in Mirone suite (Luis, 2007). Assuming that water is an incompressible fluid we translate the sea bottom deformation to the initial sea surface deformation and set the velocity field to zero for the time instant t = 0 s. We run the model for 10-hour propagation time to ensure that the tsunami reaches all observation points.

We compute the offshore wave heights for points located close to the observation points (Fig. 1) using Virtual Tide Gauges (VTG). We include the coordinates and depths of the VTG in the tables 3 and 4 in section 5. For transatlantic propagation, we consider the Coriolis effect in the tsunami simulation. We checked ~~A~~all tsunami simulations ~~were checked~~ against historical data.

For the locations in Ireland, the United Kingdom, the Azores, Madeira and Barbados we use the approximation according to the Greens Law (Green, 1838). The Greens Law is based on the linear shallow water wave equations and allows to quickly approximate the amplification of wave heights at a shallower depth close to the shore when considering a plane beach. The wave height increases to the fourth root of the ratio between the depth at the shore and the water depth at the VTG. We extrapolate the maximum wave height values between the depths of the VTG (table 3 and 4) to points located at 5 m depth.

$$h_s = \sqrt[4]{\frac{d_s}{d_d}} * h_d \qquad \text{Eq. (1)}$$

Formatted: English (United Kingdom)
Formatted: English (United Kingdom)
Formatted: English (United Kingdom)
Formatted: English (United Kingdom)
Formatted: English (United Kingdom)
Formatted: English (United Kingdom)
Formatted: English (United Kingdom)
Formatted: English (United Kingdom)
Formatted: English (United Kingdom)
Formatted: English (United Kingdom)
Formatted: English (United Kingdom)
Formatted: English (United Kingdom)
Formatted: English (United Kingdom)
Formatted: English (United Kingdom)
Formatted: English (United Kingdom)
Formatted: English (United Kingdom)
Formatted: English (United Kingdom)
Formatted: English (United Kingdom)

Where h_s and h_d are the wave heights at the shore and the VTG respectively, and d_s and d_d are the depths at the shore and the VTG respectively. For d_s we use a constant value of 5 m. the results of the approximation according to the Greens Law are presented in table 3 and 4.

4.2 Testing the hypothesis

In the 20th century, two strong magnitude earthquakes occurred in the Gloria Fault (GF) area. In view Because of this, we tested the compatibility of the tsunami observations in 1761 with the tsunamis produced by the earthquakes of the 25th November 1941 (Lynnes and Ruff, 1985; Baptista et al., 2016) and 26th May 1975 (Kaabouben et al., 2009). We use the fault plane parameters and rupture mechanism presented in Baptista et al. (2016) and Kaabouben et al. (2008) for the 1941 and 1975 events respectively. The fault dimensions and slip were made compatible with an 8.5 magnitude event using the scaling laws proposed by Wells and Coppersmith (1994), Manighetti et al. (2007), and Blaser et al. (2010) and Matias et al. (2013). These two events produce less than one-meter wave height in the North East Atlantic and were barely observed wave in the Caribbean Islands (Baptista et al., 2016; 2017). Moreover, the epicenteres of the 25th November 1941 and 26th May 1975 are located outside the area determined by Baptista et al. (2006). As expected, the TTTs do not agree with those reported in 1761,; therefore we excluded the GF as a candidate source for the 1761 event and do not consider their results for discussion.

The candidate fault area is centered at 12.00 W, 35.00 N to the west of the large NE/SW striking compressive structures (Martíinez-Loriente et al., 2013) and 85 km northeast of the epicentere, suggested by Baptista et al. (2006) (Fig. 3). We considered the fact that the historical accounts indicate an earthquake and tsunami less violent than the in 1755. To account for this, we used the fault dimensions presented in table 2 corresponding to a magnitude 8.4-8.5 earthquake (Baptista et al., 2006);, consequently, the wave heights in Lisbon and Cadiz are smaller than those observed in the 1755 tsunami (Baptista et al., 1998). The fault dimensions (length and width) presented in table 2 are compatible with the scaling laws of Wells and Coppersmith (1994), Manighetti et al. (2007), and Blaser et al. (2010) and Matias et al. (2013).

Hypotheses A and A-MS: Here we use a strike angle compatible with the study by Martíinez-Loriente et al., (2013) that follows the morphology of the Coral Patch scarp and seamount (Fig. 1 and Fig. 3). To take into account the tectonic regime of the source area we choose fault plane parameters compatible with a structure of compressive nature. The velocity vector predicted by NUVEL 1A (Fig. 3) together with the short tsunami wave periods (4-12 minutes) reported in 1761 (table 1) are in line with the mean chosen dip angle of 40 degrees (table 2). On the other hand, Martínez-Loriente et al. (2013) suggest for the Coral Patch Faults dip angles of 30±5 degrees dip and a rake angle of 90 degrees. These authors also conclude that the fault root is between 7 and 13 km depth.ed by Martinez-Loriente et al. (2013) (table 2). We approximate the rake angle according to the difference between the convergence arrow given by the circle around the Euler Pole and the fault plane (Fig. 3).

The wave period in Lisbon produced by this candidate source is 30 minutes. This value it is not compatible with the observations (Table 1). To solve this problem, we implemented a multi-segment fault here called A-MS. This multi-segment solution consists of four4 segments each 50 km. The four4 segments are placed adjacent to each other, and the rupture mechanism is equal for each segment as in hypothesis A with a mean slip of 11 m (Table 2). The slip of each segment is presented in table 2.

The synthetic waveforms are presented in figure 5 and discussed in sections 5 and 6.

Hypothesis B: Finally, we test an alternative hypothesis here called B with a ~~larger~~larger strike-slip component compared to hypothesis A. This also results in larger fault length and a steeper dip angle. Here, we consider a rupture along a fault plane rotated about 180° when compared to hypothesis A. To do this, we selected compatible strike and rake angles that result~~s~~ in a sinistral inverse lateral rupture (table 2).

The synthetic waveforms are presented in figure 7 and discussed in sections 5 and 6.

Table 2. The fault dimensions and parameters used herein to investigate candidate sources of 1761 event. We describe hypotheses (Hyp.) A-MS, A and B by the fault parameters length (L), width (W), strike, dip, rake, slip and depth. The slip values for hypothesis A-MS are listed for each segment from west to east. Additionally, we present the moment magnitude (Mag.), the assumed shear modulus (μ) and the focal mechanism.

Scenario	L [km]	W [km]	Strike [°]	Dip [°]	Rake [°]	Slip [m]	Depth [km]	Mag.	μ [Pa]	Focal mechanism
Hyp. A-MS	4 x 50	50	76	40	135	7/15/15/8	10	8.4	$4*10^{10}$	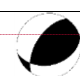
Hyp. A	200	50	76	40	135	11	10	8.4	$4*10^{10}$	
Hyp. B	280	50	254.5	70	45	15	10	8.5	$4*10^{10}$	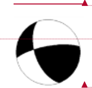

5. Results

We present the results of hypothesis A-MS and B. Hypothesis A-MS has a more significant inverse component compared to hypothesis B. Once the results of hypotheses A and A-MS produce ~~equal~~ same wave height values, but the latter produces shorter periods, ~~so~~ we opt to present the results for hypothesis A-MS. Figures 4-7 show the maximum wave height and the synthetic tsunami at the virtual tide gauges (VTG) computed offshore of each observation point of hypothesis A-MS and B. Tables 3 and 4 summari~~z~~se these results. The wave height, as mentioned in section 3, represents the maximum positive amplitude above the still water level, which is set to be 0 in the tsunami simulation. Table 3 and 4 present ~~T~~the geographical coordinates and depths of the VTGs ~~are given in tables 3 and 4~~. To compare the synthetic wave heights with the observations for the locations in Mount's Bay, Scilly Islands, Kinsale, Dungarvan, Azores, Madeira and Barbados we used the Green's Law (Green, 1838) to extrapolate the wave height values for the maximum wave between the depths of the VTG to points located at 5 m depth. For Lisbon and Cadiz, where high-resolution bathymetry is available we used two sets of nested grids and computed the tsunami inundation. Here the VTGs are located close to the shore, and the application of the Green's Law is not necessary.

5.1 Hypothesis A-MS

Figures 4 and 5 show the distribution of the maximum wave height and the respective synthetic tsunami records for hypothesis A-MS.

Analysis of figure 4 shows wave heights exceeding 4 m in the Gulf of Cadiz. At some points along the coast of Morocco maximum wave heights are about 5 m. In Great Britain, at the Scilly Islands and Mount´s Bay maximum wave heights vary between 1.7 and 1.9 m. Along the south coast of Ireland, in Kinsale and Dungarvan the tsunami simulation predicts a 1 m maximum wave height. At the eastern coast of Madeira Island, the wave heights reach 1 m whereas on the southern part of the island the wave heights are smaller. At the Azores close to Terceira Island wave heights are slightly higher than 2.5 m along the south coast of the island. The wave heights in the south of Barbados reach 0.5 m.

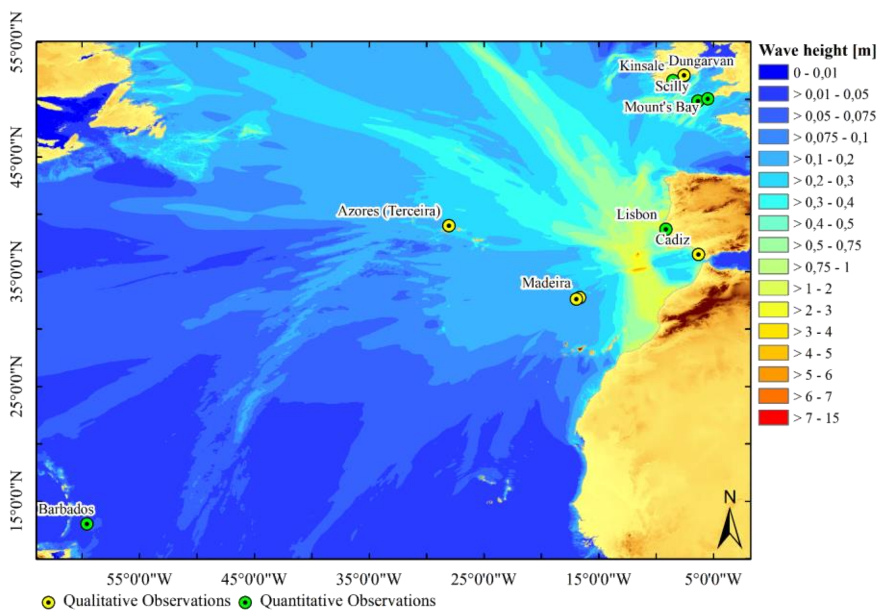

Figure 4. Maximum wave height distribution (colour scale in m) in the Atlantic basin produced by the source of hypothesis A-MS.

Formatted: English (United Kingdom)

Formatted: English (United Kingdom)

In Lisbon, the synthetic waveform shows a first peak of 1.4 m with a maximum value close to 1.8 m for the third wave, after two hours and twenty minutes of tsunami propagation. The TTT to Lisbon is 1 hour and 10 minutes and the first wave has a period of 20–25 minutes (T~~t~~able 3 and Fig. 5 (a)). In Cadiz, the synthetic tsunami waveform shows a drawdown 1 hour after the earthquake with a negative amplitude of 0.6 m and a maximum wave height of 2.4 m (table 3 and Fig. 5 (a)). The Scilly Islands synthetic tsunami waveform shows a TTT of 4 hours and a maximum peak exceeding 0.4 m with ~~a~~ 15 ~~-~~minutes period. In Mount´s Bay, TTT is 4 hours and 30 minutes and the maximum wave height is 0.5 m with 15 minutes period. In Kinsale, the tsunami model computes a TTT of 4 hours and 15 minutes. The maximum wave height there is about 0.5 m with a period shorter than 15 minutes. In Dungarvan, the tsunami arrives 5 hours after the earthquake. All VTGs in northern Europe recorded the first wave as leading elevation wave (Fig. 5 (b and c)).

Formatted: English (United Kingdom)

Formatted: English (United Kingdom)

Formatted: English (United Kingdom)

Formatted: English (United Kingdom)

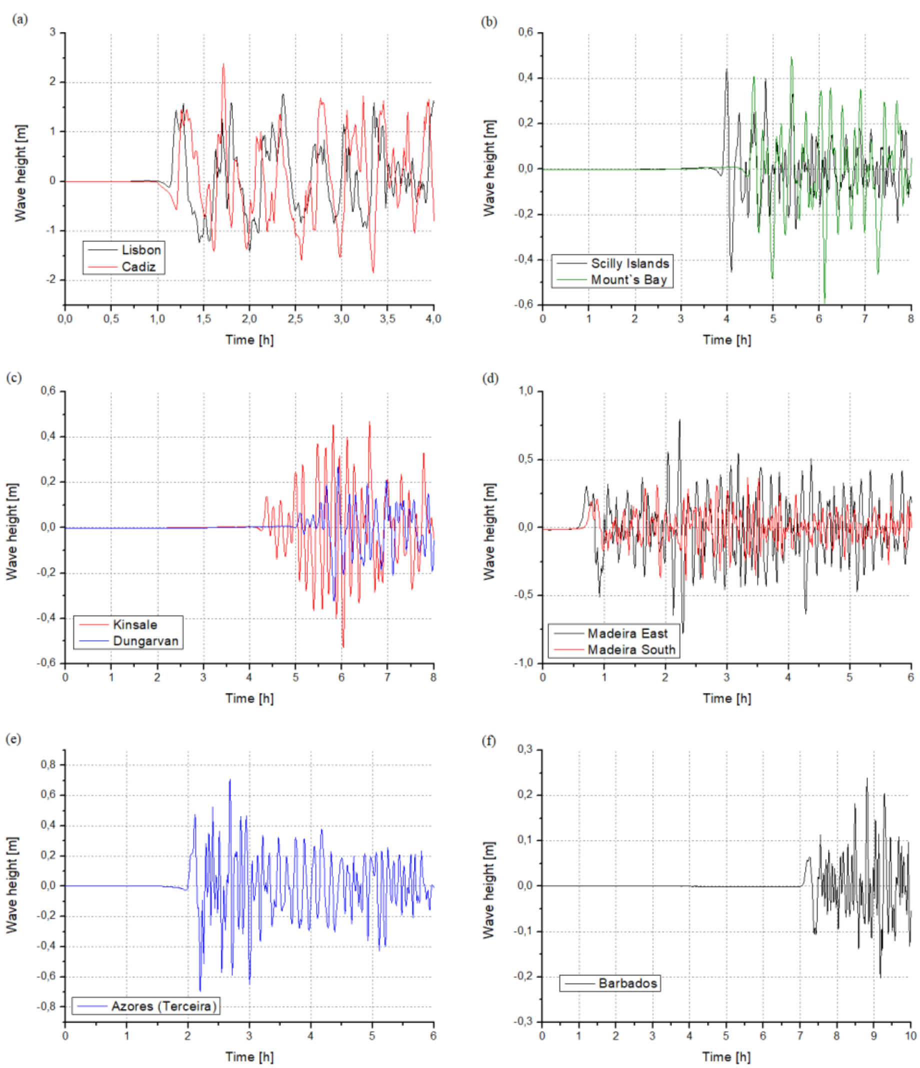

Figure 5. VTG records for hypothesis A-MS at the coordinates of the locations presented in table 3.

Formatted: English (United Kingdom)

In Madeira, hypothesis A-MS produces maximum wave heights at the VTG of 0.8 m in the eastern part of the island and about 0.4 m, in the southern part; the TTT to the east and southern coast of the island is half an hour and 40 min respectively (Fig. 5 (d)). In the Azores, close to the island of Terceira, the wave heights reach approximately 0.7m (Fig. 5 (e)).

In Barbados, hypothesis A-MS produces the first wave of about 0.1 m after about 7 hours with about 30 minutes period. Only after 9 hours and 30 minutes, the wave height exceeds 0.2 m (Fig. 5(f)).

We applied the Green's Law in all locations except Lisbon and Cadiz to extrapolate the maximum wave height values to a depth of 5 m close to the shore to compare the values with the observations in section 3. We present t~~T~~he maximum wave height values after application of Green's Law ~~are presented~~ in table 3.

Formatted: English (United Kingdom)

Table 3. Results of the VTGs for hypothesis A-MS. The column TTT lists the observed Tsunami Travel Times. The column polarity indicates the first movement of the sea upward (U) or downward (D).

Local		VTG coordinates & depth			TTT	Wave height [m]				Polarity	Period
		Lon. [°]	Lat. [°]	d [m]		First	max.	Green's Law	Obs.		
Lisbon		-9.136	38.706	3	~ 1 h 10 min	1.6 m	1.8 m	nesting	1.2 – 1.8 m	D	< 30 min
Cadiz		-6.291	36.524	4	~ 1 h	-0.6 m	2.4 m	nesting	-	D	~ 30 min
Scilly Islands		-06.383	49.85	50	~ 4 h	0.4 m	0.4 m	0.7 m	0.6 – 1.2 m	U	~ 15 min
Mount´s Bay		-05.48	50.08	26	~ 4 h 30 min	0.4 m	0.5 m	0.8 m	1.2 – 1.8 m	U	~ 15 min
Kinsale		-08.500	51.653	28	~ 4 h 15 min	0.1 m	0.5 m	0.8 m	0.6 m	U	< 15 min
Dungarvan		-07.479	51.949	50	~ 5 h	0.1 m	0.3 m	0.5 m	-	U	< 15 min
Madeira	**E**	-16.666	32.750	51	~ 30 min	0.3 m	0.8 m	1.4 m	-	U	~ 30 min
	S	-16.926	32.619	51	~ 40 min	0.2 m	0.4 m	0.7 m	-	U	~ 30 min
Azores		-27.150	38.800	53	~ 2 h	0.5 m	0.7 m	1.3 m	-	U	~ 15 min
Barbados		-59.566	13.033	50	~ 7 h	0.1 m	0.2 m	0.4 m	0.45 – 0.6 m	U	~ 30 min

Formatted: English (United Kingdom)

5.2 Hypothesis B

In h~~H~~ypothesis B the dip angle was increased relative to hypothesis A resulting in the dominant strike-slip mechanism. In figure 6, we depict the maximum wave height for option B.

Analy~~z~~sing figure 6 we find maximum wave heights of 15 m along the coast of Morocco. In the Gulf of Cadiz, the wave heights do not exceed 2 m. In Great Britain, at the Scilly Islands the maximum wave height is close to 2.3 m, and in Mount´s Bay, the maximum wave height values reach 1.8 m. For the locations in Ireland, Kinsale and Dungarvan, the maximum wave heights exceed 1.4 m. The eastern part of Madeira experiences wave heights greater than 2.5 m, decreasing towards the southern parts of the Island (Fig. 6). The maximum wave height exceeds 5.5 m on the eastern side of the island of Terceira in the Azores. For Barbados, this source computes maximum wave heights exceeding 0.7 m.

Formatted: English (United Kingdom)

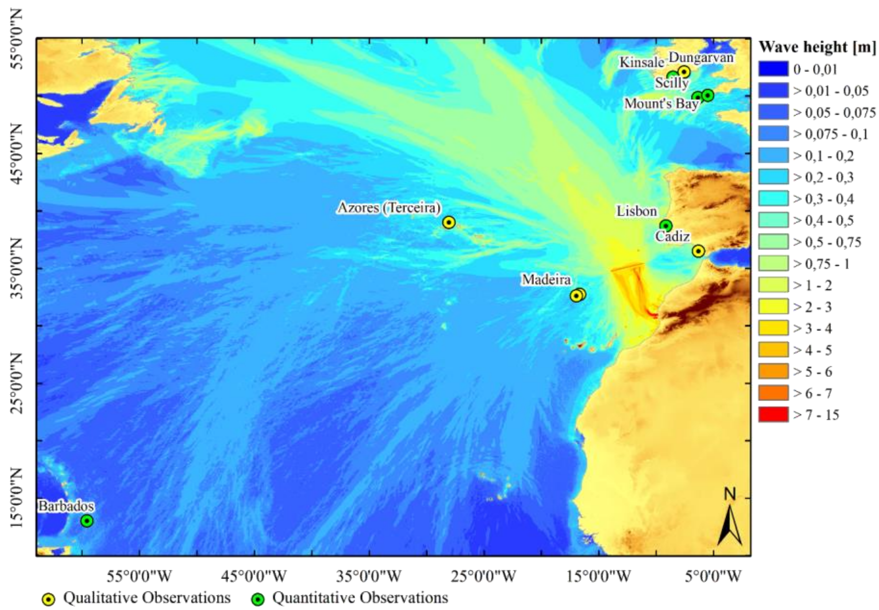

Figure 6. Maximum wave height distribution (colour scale in m) in the Atlantic basin produced by the source of hypothesis B.

Figure 7 presents the corresponding synthetic tsunami waveforms at the VTGs. Table 4 gives a summary of the results. The analysis of the synthetic waveforms shows that a small withdraw of about 0.2 m arrives in Lisbon after 1 hour and 15 minutes followed by a water surface elevation of 0.9 m. The third wave has a maximum positive amplitude of 2.2 m (Fig. 7 (a)).

The maximum wave heights at the Scilly Islands is 0.5 m (Fig. 7 (b)). The first wave reaches 0.4 m, arriving close to 4 h after the earthquake. The synthetic tsunami waveform shows around 15-minute wave period. In Mount`s Bay, the first wave of 0.4 m arrives after 4 hours and 30 minutes with a 15-minute wave period (Fig. 7 (b)). Here, the maximum wave height, 0.7 m, comes more than 6 hours after the earthquake. In Kinsale, hypothesis B produces a maximum wave height of 0.6 m. The first wave of 0.2 m wave height in the VTG arrives after 4 hours and 15 minutes of tsunami propagation; here, the period is shorter than 15 min (Fig. 7 (c)).

In Madeira, the first and the maximum wave heights are greater in the eastern part of the island compared to the southern part. Maximum wave heights values reach 1.4 m in the east part of Madeira and 1.1 m in the south part of Madeira (Fig. 7 (d)). In the Azores, the wave height for Terceira island reaches up to 2.4 m (Fig. 7 (e)).

Formatted: English (United Kingdom)

Formatted: English (United Kingdom)

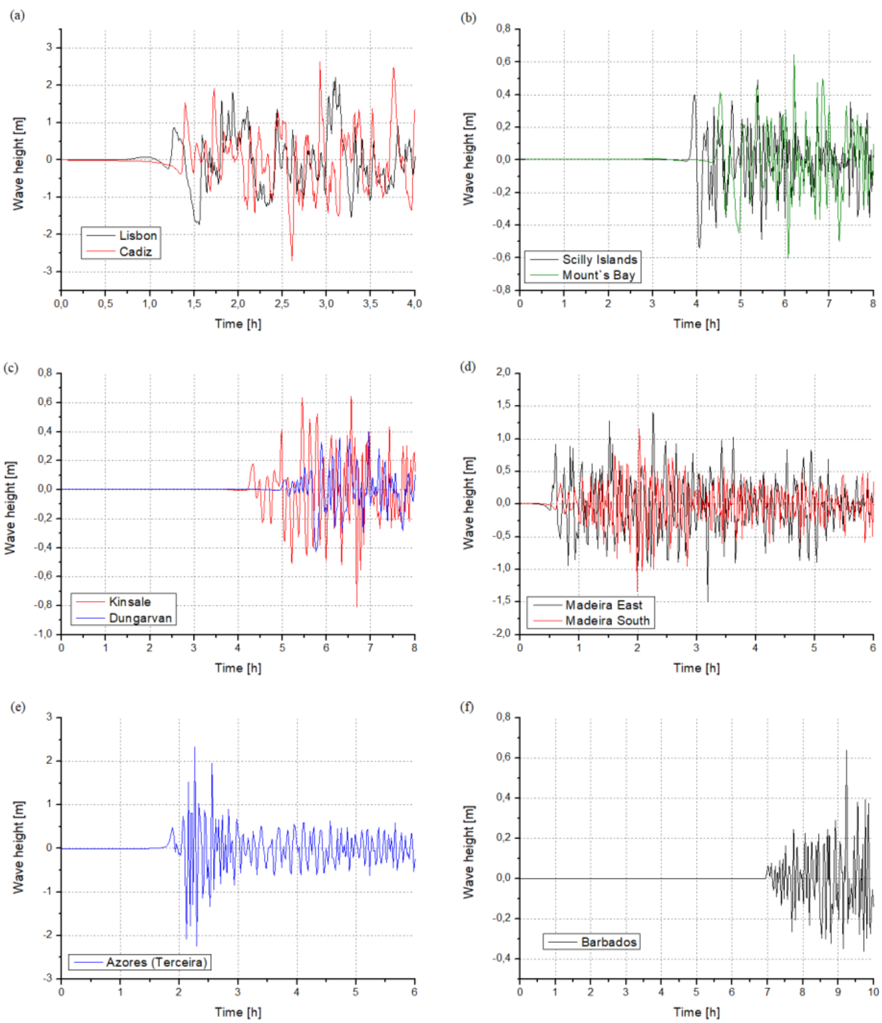

Figure 7. VTG records for hypothesis B at the coordinates of the locations presented in table 4.

Formatted: English (United Kingdom)

Hypothesis B predicts a tsunami travel time of 7 hours to Barbados with the first peak of less than 0.1m and a maximum peak of 0.6 m after 9 hours and 15 minutes (Fig. 7 (f)). The first wave has a period slightly below 15 minutes. Table 4 gives a summary of the results for hypothesis B.

We also applied the Green's Law for this solution. We present ~~T~~the maximum wave height values after application of Green's Law in table 4~~ are presented in table 4~~.

Table 4. Results of the VTGs for hypothesis B. The column TTT lists the observed Tsunami Travel Times. The column polarity indicates the first movement of the sea upward (U) or downward (D).

Local		VTG coordinates & depth Lon. [°]	Lat. [°]	d [m]	TTT	Wave height [m] First	max.	Green's Law	Obs.	Polarity	Period
Lisbon		-9.136	38.706	3	~ 1 h 15 min	0.9 m	2.2 m	nesting	1.2 – 1.8 m	D	> 30 min
Cadiz		-6.291	36.524	4	~ 1 h	-0.4 m	2.6 m	nesting	-	D	~ 30 min
Scilly Islands		-06.383	49.85	50	< 4 h min	0.4 m	0.5 m	0.9 m	0.6 – 1.2 m	U	~ 15 min
Mount´s Bay		-05.48	50.08	26	~ 4 h 30 min	0.4 m	0.7 m	1 m	1.2 – 1.8 m	U	~ 15 min
Kinsale		-08.500	51.653	28	~ 4 h 15 min	0.2 m	0.6 m	1 m	0.6 m	U	< 15 min
Dungarvan		-07.479	51.949	50	~ 5 h	0.1 m	0.4 m	0.7 m	-	U	< 15 min
Madeira	**E**	-16.666	32.750	51	~ 30 min	0.9 m	1.4 m	2.5 m	-	U	~ 30 min
	S	-16.926	32.619	51	~ 40 min	0.3 m	1.1 m	2.1 m	-	U	~ 30 min
Azores		-27.150	38.800	53	~ 1 h 45 min	0.5 m	2.4 m	4.2 m	-	U	~ 15 min
Barbados		-59.566	13.033	50	~ 7 h	0.1 m	0.6 m	1.1 m	0.45 – 0.6 m	U	~ 30 min

6. Discussion ~~and Conclusion~~

We investigated possible sources of the earthquake and tsunami on the 31st March 1761 earthquake in the Atlantic.

Firstly, we excluded the locations similar to the instrumental events of the 20th century: 25.11.1941 (Baptista et al., 2016) and 26.05.1975 (Kaabouben et al., 2009) because of incompatibility of tsunami travel times (Fig.2).

Secondly, we placed a source about 85 km to the east of the location proposed by Baptista et al. (2006) ~~to include the Barbados travel time in our dataset~~ (Fig. 2).

After setting the source position, we investigated focal mechanisms for the parent earthquake. We selected two focal mechanisms for testing: A and B. Solution A-MS corresponds to focal mechanism A with a multi-segment fault plane as described in section 4.2 (table 2).

Our tests produce a set of TTTs compatible with the observations; Maximum differences between observed and predicted travel times are 15 minutes in the near-field and 30 minutes in the far-field, ~~with a 15-minute delay in the near-field and 30-minute delay in the far-field.~~ These differences are acceptable considering that the exact location of the observation points is

Formatted: English (United Kingdom)
Formatted: English (United Kingdom)
Formatted: English (United Kingdom)
Formatted: English (United Kingdom)
Formatted: English (United Kingdom)
Formatted: English (United Kingdom)
Formatted: English (United Kingdom)

unknown. ~~These~~ Travel time results are valid for A, B and A-MS as the locations are ~~similar~~ the same. Tables 3 and 4 show that the predicted travel times are compatible with a source located in the area west- of the Coral Patch.

Any source located in the Northeast Atlantic south of the Scilly islands produces a shorter tsunami travel time to Scilly island than Mount's Bay. This fact shows that the~~e~~ 6 hours TTT reported in Kinsale contradicts the 4 hours TTT reported for Dungarvan (Fig. 1). On the other hand, the tsunami travel times predicted by our numerical simulation are consistent with their ~~relative geographical~~ position related to the source area. ~~-~~ The proposed

source~~Source~~ A produces wave heights applying the Green's Law to the values recorded at the VTGs which are compatible with the observations in Lisbon, Kinsale, Scilly and Barbados (Fig. 5 and table 3). The results of the synthetic wave records of Dungarvan, Madeira and the Azores are compatible with the observations. In Mount's Bay, the wave height computed using the Green's Law of the VTG value is smaller than the one reported. However, analysis of figure 4 shows that the computed maximum wave heights greater than 1.6 m for Mount's Bay. This value agrees with the observation.

The proposed source ~~Source~~ B produces wave heights compatible with the observation in Lisbon, Scilly and Mount's Bay. We apply the Green's Law (Eq. 1) using the wave heights recorded at the VTG in Kinsale and Barbados and obtain larger wave heights than reported (table 4). Also, the ~~modelled~~ computed maximum wave heights in figure 6 are higher than 1.4 m, 2.2 m and 0.7 m for Kinsale, Scilly and Barbados respectively. These values are higher than the one observed. At the Azores, the wave height reaches 4.2 m (table 4); however, the descriptions do not report an inundation. Also, at the coast of Morocco, source B predicts wave heights close to 14 m. To our knowledge, the historical documents do not report any abnormal movement of the sea in Morocco.

The observations do not account for inundation in Lisbon. To investigate this fact, we estimated the tide condition in Lisbon for the 31st March 1761~~is~~ day. To do this, we used a Moon Phase table (USNO, 2017) and concluded that the tide was 2.6 m above hydrographic zero (HZ) (in dropping tide conditions) at 1 p.m. on the 31st of March 1761 (table 5).

The maximum of the synthetic wave record for source A is 1.8 m about 2 hours and 15 minutes when the tide has dropped underneath 2.3 m above HZ. Adding 1.8 m to 2.3 m, we obtain 4.1m; this value is less than the tide amplitude in spring tide condition. Considering that Lisbon downtown was rebuilt 3 m above sea level after the 1755 event (Baptista et al., 2011) the predicted wave heights are compatible with no flooding.

~~Source~~ The proposed source B ~~produces a first wave of 0.9~~generates for the first wave height 0.9 m but a maximum wave height of 2.2 m. The maximum wave height occurs at 15:00 o'clock and the estimated tide is approximately 2.1 m above HZ. Adding 2.2 to 2.1 we reach spring tide condition of 4.3 m.

Given the considerations above the tide, analysis favours solution A.

Table 5. Tide levels at the time of the earthquake and tsunami arrival.

	~~Time~~	~~Tide condition~~	~~Estimated height relative to Hydrographic Zero~~
~~Earthquake~~	~~Noon~~	~~Full tide~~	~~2.9 m~~
~~Tsunami arrival time~~	~~13:15~~	~~Dropping tide~~	~~2.6 m~~

Formatted: English (United Kingdom)
Formatted: English (United Kingdom)
Formatted: English (United Kingdom)
Formatted: English (United Kingdom)
Formatted: English (United Kingdom)
Formatted: Not Highlight
Formatted: English (United Kingdom)
Formatted: Not Highlight
Formatted: English (United Kingdom)
Formatted: English (United Kingdom)
Formatted: English (United Kingdom)
Formatted: English (United Kingdom)
Formatted: English (United Kingdom)
Formatted: English (United Kingdom)
Formatted: English (United Kingdom)
Formatted Table

~~Max. wave height Hyp. AMS~~	~~14:15~~	~~Dropping tide~~	~~2.3 m~~
~~Max. wave height Hyp. B~~	~~15:00~~	~~Dropping tide~~	~~2.1 m~~
	~~Time~~	~~Tide condition~~	~~Estimated height relative to Hydrographic Zero~~
~~**Earthquake**~~	~~Noon~~	~~Full tide~~	~~2.9 m~~
~~**Tsunami arrival time**~~	~~13:15~~	~~Dropping tide~~	~~2.6 m~~
~~**Max. wave height Hyp. AMS**~~	~~14:15~~	~~Dropping tide~~	~~2.3 m~~
~~**Max. wave height Hyp. B**~~	~~15:00~~	~~Dropping tide~~	~~2.1 m~~
	Time	**Tide condition**	**Estimated height relative to Hydrographic Zero**
Earthquake	Noon	Full tide	2.9 m
Tsunami arrival time	13:15	Dropping tide	2.6 m
Max. wave height Hyp. AMS	14:15	Dropping tide	2.3 m
Max. wave height Hyp. B	15:00	Dropping tide	2.1 m

The tidal range in Barbados is about 1 m. This small range might favour the observability of small first waves at tsunami arrival. For source ~~source~~ A, the first wave in Barbados is about 0.1 m which raises the question if people might have noticed the advance of the sea. Close to 9 o'clock, 2 hours after tsunami arrival, the positive peak in~~at~~ the VTG is higher than 0.2 m which results in 0.4 m when estimating the wave height applying the Green's Law for 5 m depth close to the shore. The coeval sources report similar wave height values.

Also, for source B, the wave height is smaller than 0.1 m at the VTG at the time of tsunami arrival. About 45 minutes later the waves are large than 0.2 m. The maximum peak occurs ca. 2 hours after tsunami arrival at 9 o'clock. Because of ~~T~~ the small tide amplitude in Barbados does not contribute to select among the two candidate sources.

The summary (Annual register, 1761) states that the waves seemed to abate but at 10 o'clock started again with higher intensity and lasted until the next morning - t~~. T~~his observation of greater amplitudes some hours after tsunami arrival fits for both sources. However, the timings of increasing wave heights do not match.

In Cadiz, both sources produce the observed withdrawal. Both~~In~~ sources, A and B predict a drawdown of 0.6 m and 0.4 m respectively. High tide in Cadiz is about 1 hour earlier than in Lisbon. Once the tide was in dropping conditions at the time of the tsunami arrival a larger drawdown is more likely to be observed.

Considering the points discussed above, we conclude our preferred solution is A-MS. Following facts justify our choice:

• The candidate source in hypothesis A-MS is compatible with the geodynamic setting predicted by the NUVEL 1A model (DeMets et al., 1999). NE/SW compressive structures with ~~similar~~comparable fault plane parameters have been identified close to the Coral Patch seamount (Fig. 1 and 3). The proposed structure is possibly propagating and reactivating the NE-SW striking oceanic rifting fabric towards the epicentre suggested by Baptista et al. (2006). Nevertheless, we must stress that

Formatted: English (United Kingdom)
Formatted: English (United Kingdom)
Formatted: English (United Kingdom)
Formatted: English (United Kingdom)
Formatted: English (United Kingdom)
Formatted: Font: Bold
Formatted: English (United Kingdom)
Formatted: English (United Kingdom)
Formatted: English (United Kingdom)
Formatted: English (United Kingdom)
Formatted: English (United Kingdom)
Formatted: English (United Kingdom)
Formatted: English (United Kingdom)
Formatted: English (United Kingdom)
Formatted: English (United Kingdom)
Formatted: English (United Kingdom)

~~(~~Martí~~i~~nez-Loriente et al.~~,~~ (2013) do not suggest an extension of the seismogenic structure at the CPF although no detailed multi-channel seismic survey has been carried out to the west of the CPF in the proposed source area.)~~.~~

• The wave heights produced by the numerical models are in better agreement with ~~hypothesis~~ proposed source A-MS.

• Wave heights greater than 14 m produced by hypothesis~~solution~~ B would result in a catastrophic scenario which is rather unlikely and nor observed neither or reported. Also, 4.2 m wave height produced by hypothesis B in the Azores would have caused inundation, which has not been reported.

• Although both solutions follow our considerations for Lisbon, the wave heights generated by source A-MS seem ~~more reasonable~~ to be more comparable ~~and close~~ to the observed fluctuation of 2.4 m than the wave heights produced by source B.

• The larger drawdown in Cadiz favours solution A-MS.

The reassessment of the reports of Barbados and Cadiz support the choice selected here. While the tsunami travel time for Barbados supports the source location, the fact that there was no inundation reports in Cadiz supports the magnitude and rupture mechanism proposed here.

7. Conclusion

• The source proposed here for the 1761 event is compatible with the tsunami observation dataset, the macro-seismic intensity data (Baptista et al., 2006) and with the geodynamic context of the area predicted by the kinematic plate model NUVEL 1-A.

~~• The re-evaluated TTT for Barbados is consistent with the source location proposed here.~~

• The ~~tectonic~~ source~~source~~ proposed here ~~to reproduce the observations of the 31st March 1761 tsunami~~ is located ~~southwest of the source of the 1st November 1755 event~~ in the SWIM, an area of widespread compressive structures (Hayward et al., 1999), corresponding to a fault that extends from the western segment of the CPF towards the epicentre proposed by Baptista et al. (2006).

The investigation of each historical event in the area contributes to a better understanding of the structure of this diffuse plate boundary and ultimately leads to a better evaluation of the seismic and tsunami hazard.

This study together with the study by Baptista et al. (2006) underlines the need to include the 1761 event in all seismic and tsunami hazard assessments in the Northeast Atlantic basin.

Acknowledgements. This work is funded by FCT (Instituto Dom Luiz; FCT PhD grant ref. **PD/BD/135070/2017**). The authors wish to thank the editor Ira Didenkulova ~~and~~ and the reviewers Uri S. ten Brink, ~~and~~ Ceren Özer Sözdinler and Sara Martínez-Loriente for their constructive comments and suggestions that greatly helped to improve this manuscript. Finally, the authors wish to thank Pedro Terrinha for his valuable advice and interesting discussions on the geological context of the area and Paul-Louis Blanc for the translation of the report in Journal Historique (1773).

Formatted: English (United Kingdom)
Formatted: English (United Kingdom)
Formatted: English (United Kingdom)
Formatted: English (United Kingdom)
Formatted: English (United Kingdom)
Formatted: Heading 1
Formatted: English (United Kingdom)
Formatted: Font color: Auto, English (United Kingdom)
Formatted: English (United Kingdom)
Formatted: English (United Kingdom)
Formatted: English (United Kingdom)
Formatted: English (United Kingdom)
Formatted: English (United Kingdom)
Formatted: English (United Kingdom)
Formatted: English (United Kingdom)
Formatted: English (United Kingdom)

References

Annual Register: Volume 4, pages 92-95, 1761.

Argus, D. F., Gordon, R. G., DeMets, C., and Stein, S.: Closure of the Africa-Eurasia-North America plate motion circuit and tectonics of the Gloria fault. Journal of Geophysical Research: Solid Earth, 94(B5), 5585-5602, doi:10.1029/JB094iB05p05585, 1989.

Baptista, M. A., Miranda, P. M. A., Miranda, J. M., and Victor, L. M.: Constrains on the source of the 1755 Lisbon tsunami inferred from numerical modelling of historical data on the source of the 1755 Lisbon tsunami, Journal of Geodynamics, 25(1-2), 159-174, https://doi.org/10.1016/S0264-3707(97)00020-3, 1998a.

Baptista, M. A., Heitor, S., Miranda, J. M., Miranda, P., and Victor, L. M.: The 1755 Lisbon tsunami; evaluation of the tsunami parameters. Journal of Geodynamics, *25*(1-2), 143-157, 1998b.

Baptista, M. A., Miranda, J. M., Chierici, F., and Zitellini, N.: New study of the 1755 earthquake source based on multi-channel seismic survey data and tsunami modeling, Nat. Hazards Earth Syst. Sci., 3, 333-340, https://doi.org/10.5194/nhess-3-333-2003, 2003.

Baptista, M. A., Miranda, J. M., and Luis, J. F.: In search of the 31 March 1761 earthquake and tsunami source, Bulletin of the Seismological Society of America, 96(2), 713-7211, doi:10.1785/0120050111, 2006.

Baptista, M. A., Miranda, J. M., Lopes, F. C., and Luis, J. F.: The source of the 1722 Algarve earthquake: evidence from MCS and Tsunami data. Journal of Seismology, 11(4), 371-380, https://doi.org/10.1007/s10950-007-9058-y, 2007.

Baptista, M. A. and Miranda, J. M.: Revision of the Portuguese catalog of tsunamis, Nat. Hazards Earth Syst. Sci., 9, 25-42, https://doi.org/10.5194/nhess-9-25-2009, 2009.

Baptista, M. A., Miranda, J. M., Batlló, J., Lisboa, F., Luis, J., and Maciá, R.: New study on the 1941 Gloria Fault earthquake and tsunami, Nat. Hazards Earth Syst. Sci., 16, 1967-1977, https://doi.org/10.5194/nhess-16-1967-2016, 2016.

Baptista, M. A., Miranda, J. M., Matias, L., and Omira, R.: Synthetic Tsunami Waveform Catalogs With Kinematic Constraints, Nat. Hazards Earth Syst. Sci. Discuss., https://doi.org/10.5194/nhess-2017-57, 2017.

Barkan, R., Uri, S., and Lin, J.: Far field tsunami simulations of the 1755 Lisbon earthquake: Implications for tsunami hazard to the US East Coast and the Caribbean, Marine Geology, 264(1-2), 109-122, https://doi.org/10.1016/j.margeo.2008.10.010, 2009.

Bartolome, R., Gràcia, E., Stich, D., Martínez-Loriente, S., Klaeschen, D., de Lis Mancilla, F., Lo Iacono, C., Dañobeitia, J. J. and Zitellini, N.: Evidence for active strike-slip faulting along the Eurasia-Africa convergence zone: Implications for seismic hazard in the southwest Iberian margin. Geology, 40(6), 495-498, 2012.

Bellin, J. N.: Carte hydrographique de La Baye De Cadix. 1762.

~~Blanc, P. L.: The tsunami in Cadiz on 1 November 1755: A critical analysis of reports by Antonio de Ulloa and by Louis Godin, Comptes Rendus Geoscience, 340(4), 251-261, https://doi.org/10.1016/j.crte.2007.12.001, 2008.~~

Formatted: English (United Kingdom)
Formatted: English (United Kingdom)
Formatted: English (United Kingdom)
Formatted: English (United Kingdom)
Formatted: English (United Kingdom)
Formatted: English (United Kingdom)
Formatted: Font: Not Italic, Portuguese (Portugal)
Formatted: Portuguese (Portugal)
Formatted: Font: Not Italic, Portuguese (Portugal)
Formatted: Portuguese (Portugal)
Formatted: Not Highlight
Formatted: Portuguese (Portugal)
Formatted: Not Highlight
Formatted: Portuguese (Portugal)
Formatted: English (United Kingdom)
Formatted: English (United Kingdom)
Formatted: English (United Kingdom)

Blaser, L., Krüger, F., Ohrnberger, M., and Scherbaum, F.: Scaling relations of earthquake source parameter estimates with special focus on subduction environment, Bulletin of the Seismological Society of America, 100(6), 2914-2926, https://doi.org/10.1785/0120100111, 2010.

Borlase, W.: Some Account of the extraordinary Agitation of the Waters in Mount's-bay, and other Places, on the 31st of March 1761: In a Letter for the Reverend Dr. C Lyttelton, Philosophical Transactions of the Royal Society, vol. 52, Page 418-431, 1762.

Custódio, S., Dias, N. A., Carrilho, F., Góngora, E., Rio, I., Marreiros, C., Morais, I., Alves, P., and Matias, L.: Earthquakes in western Iberia: Improving the understanding of lithospheric deformation in a slowly deforming region, Geophysical Journal International, 203(1), 127-145, https://doi.org/10.1093/gji/ggv285, 2015.

DeMets, C., Gordon, R. G., Argus, D. F., and Stein, S.: Current plate motions. Geophysical journal international, 101(2), 425-478, 1990.

DeMets, C., Gordon, R. G., Argus, D. F., and Stein, S.: Effect of recent revisions to the geomagnetic reversal time scale on estimates of current plate motions, Geophysical research letters, 21(20), 2191-2194, doi:10.1029/94GL02118, 1994.

DeMets, C. and Dixon, T. H.: New kinematic models for Pacific-North America motion from 3 Ma to present, I: Evidence for steady motion and biases in the NUVEL-1A model. Geophysical Research Letters, 26(13), 1921-1924, doi:10.1029/1999GL900405, 1999.

Duarte, J. C., Rosas, F. M., Terrinha, P., Schellart, W. P., Boutelier, D., Gutscher, M. A., and Ribeiro, A.: Are subduction zones invading the Atlantic? Evidence from the southwest Iberia margin, Geology, 41(8), 839-842, https://doi.org/10.1130/G34100.1, 2013.

Fearns, J.: Letter to The London Chronicle N. 731, page. 214, 1761.

Fernandes, R. M. S., Bastos, L., Miranda, J. M., Lourenço, N., Ambrosius, B. A. C., Noomen, R., and Simons, W.: Defining the plate boundaries in the Azores region, Journal of Volcanology and Geothermal Research, 156(1), 1-9, https://doi.org/10.1016/j.jvolgeores.2006.03.019, 2006.

Fernandes, R. M. S., Miranda, J. M., Meijninger, B. M. L., Bos, M. S., Noomen, R., Bastos, L., Ambrosius, B. A. C., Riva, R. E. M.: Surface velocity field of the Ibero-Maghrebian segment of the Eurasia-Nubia plate boundary. *Geophysical Journal International*, *169*(1), 315-324, 2007.

GEBCO: http://www.gebco.net, The General Bathymetric Chart of the Oceans, GEBCO_2014 grid, version 20150318, 2014, last access: 1 February 2018.

Geissler, W. H., Matias, L., Stich, D., Carrilho, F., Jokat, W., Monna, S., IbenBrahim, A. Mancilla, F., Gutscher, M.-A., Sallarès, V., Zitellini, N.: Focal mechanisms for sub–crustal earthquakes in the Gulf of Cadiz from a dense OBS deployment. Geophysical Research Letters 37, L18309, doi:10.1029/2010GL044289, 2010.

Gràcia, E., Dañobeitia, J.J., Vergés, J. and PARSIFAL Team: Mapping active faults offshore Portugal (36N– 38N): Implications for seismic hazard assessment along the southwest Iberian margin. Geology, 31(1), 83–86, 2003.

Formatted: English (United Kingdom)
Formatted: English (United Kingdom)
Formatted: English (United Kingdom)
Formatted: English (United Kingdom)
Formatted: English (United Kingdom)
Formatted: English (United Kingdom)
Formatted: English (United Kingdom), Not Highlight
Formatted: English (United Kingdom)
Formatted: English (United Kingdom), Not Highlight
Formatted: English (United Kingdom)
Formatted: English (United Kingdom), Not Highlight
Formatted: English (United Kingdom)

Green, G.: On the motion of waves in a variable canal of small depth and width. Transactions of the Cambridge Philosophical Society, 6, 457, 1838.

Gutenberg, B. and Richter, C. F.: Seismicity of the Earth and associated phenomena, Princeton University Press, Princeton, New Jersey, 1949.

Gutscher, M. A., Malod, J., Rehault, J. P., Contrucci, I., Klingelhoefer, F., Mendes-Victor, L., and Spakman, W.: Evidence for active subduction beneath Gibraltar, Geology, 30(12), 1071-1074, https://doi.org/10.1130/0091-7613(2002)030<1071:EFASBG>2.0.CO;2, 2002.

Gutscher, M. A., Baptista, M. A., and Miranda, J. M.: The Gibraltar Arc seismogenic zone (part 2): constraints on a shallow east dipping fault plane source for the 1755 Lisbon earthquake provided by tsunami modeling and seismic intensity, Tectonophysics 426.1, 153-166, https://doi.org/10.1016/j.tecto.2006.02.025, 2006.

Gutscher, M. A., Dominguez, S., Westbrook, G. K., Le Roy, P., Rosas, F., Duarte, J. C., Terrinha, P., Miranda, J. M., Graindorge, D., Sallares, V., and Bartolome, R.: The Gibraltar subduction: A decade of new geophysical data. Tectonophysics, 574, 72-91, DOI 10.1016/j.tecto.2012.08.038, 2012.

Hayward, A., Watts, A. B., Westbrook G. K., Collier J. S.: A seismic reflection and GLORIA study of compressional deformation in the Gorringe Bank region, Eastern North Atlantic. Geophysical Journal International 138, 831–850, doi:10.1046/j.1365-246x.1999.00912.x, 1999.

Heberden, T.: An Account of the Earthquake felt in the Island of Madeira, March 31, 1761. Communicated by W Heberden, Philosophical Transactions of the Royal Society, vol. 52, pag. 155, 1761.

Instituto Geográfico Nacional (IGN): http://www.ign.es/web/ign/portal/sis-catalogo-terremotos/, last access: 1 February 2018.

Jiménez-Munt, I., Fernàndez, M., Vergés, J., Afonso, J.C., Garcia-Castellanos, D., Fullea, J.: Lithospheric structure of the Gorringe Bank: Insights into its origin and tectonic evolution. Tectonics 29. doi:10.1029/2009TC002458, 2010.

Johnston, A. C.: Seismic moment assessment of earthquakes in stable continental regions—III, New Madrid 1811–1812, Charleston 1886 and Lisbon 1755, Geophysical Journal International, 126(2), 314-344, https://doi.org/10.1111/j.1365-246X.1996.tb05294.x, 1996.

Journal Historique: Suite de La Clef ou Journal Historique sur Les Matieres du Tems, contenant quelques nouvelles de Litterature, et autres Remarques curieuses, Juin 1773, Premiere Partie, Tome CXIII, Paris 462-464, 1773 (in French).

Kaabouben, F., Brahim, A. I., Toto, E., Baptista, M. A., Miranda, J. M., Soares, P., & Luis, J. F.: On the focal mechanism of the 26.05. 1975 North Atlantic event contribution from tsunami modeling. Journal of seismology, 12(4), 575-583, 2008.

Kaabouben, F., Baptista, M. A., Iben Brahim, A., El Mouraouah, A., and Toto, A.: On the moroccan tsunami catalogue, Nat. Hazards Earth Syst. Sci., 9, 1227-1236, https://doi.org/10.5194/nhess-9-1227-2009, 2009.

Laughton, A. S. and Whitmarsh, R. B.: The Azores-Gibraltar plate boundary, in: Geodynamics of Iceland and the North Atlantic area, NATO Advanced Study Institute, Reykjavik, Springer, the Netherlands, 63–81, https://doi.org/10.1007/978-94-010-2271-2_5, 1974.

Liu, P. L. F., Cho, Y. S., Briggs, M. J., Kanoglu, U., and Synolakis, C. E.: Runup of solitary waves on a circular island, Journal of Fluid Mechanics, 302, 259-285, https://doi.org/10.1017/S0022112095004095, 1995.

Liu, P. L., Woo, S. B., and Cho, Y. S.: Computer programs for tsunami propagation and inundation, Cornell University, available at: http://tsunamiportal.nacse.org/documentation/COMCOT_tech.pdf, last access: 1 February 2018, 1998.

Luis, J. F.: Mirone: A multi-purpose tool for exploring grid data, Computers & Geosciences, 33(1), 31-41, https://doi.org/10.1016/j.cageo.2006.05.005, 2007.

Lynnes, C. S. and Ruff, L. J.: Source process and tectonic implications of the great 1975 North Atlantic earthquake, Geophys. J. Int., 82, 497–510, 1985.

Mallet, Robert and John Wm. Mallet: The Earthquake Catalogue of the British Association, Transactions of the British Association for the Advancement of Science, 1852 to 1858, Reports 3 and 4, Taylor and Francis, London, 800 pp, 1858.

Manighetti, I., Campillo, M., Bouley, S., and Cotton, F.: Earthquake scaling, fault segmentation, and structural maturity. Earth and Planetary Science Letters, 253(3-4), 429-438, https://doi.org/10.1016/j.epsl.2006.11.004, 2007.

Mansinha, L. and Smylie, D. E.: The displacement fields of inclined faults, Bulletin of the Seismological Society of America, 61(5), 1433-1440. 1971.

Martínez-Loriente, S., Gràcia, E., Bartolome, R., Sallarès, V., Connors, C., Perea, H., Lo Iacono, C., Klaeschen, D., Terrinha P., Dañobeitia J. J., and Zitellini, N.: Active deformation in old oceanic lithosphere and significance for earthquake hazard: Seismic imaging of the Coral Patch Ridge area and neighboring abyssal plains (SW Iberian Margin), Geochemistry, Geophysics, Geosystems, 14(7), 2206-2231, doi:10.1002/ggge.20173, 2013.

Martínez-Loriente, S., Sallarès, V., Gràcia, E., Bartolome, R., Dañobeitia, J. J., Zitellini, N.: Seismic and gravity constraints on the nature of the basement in the Africa-Eurasia plate boundary: New insights for the geodynamic evolution of the SW Iberian Margin. Journal of Geophysical Research 119, 127-149, doi:10.1002/2013JB010476, 2014.

Martínez-Loriente, S., Gràcia, E., Bartolome, R., Perea, H., Klaeschen, D., Dañobeitia, J. J., Zitellini, N., Wynn, R. B. and Masson, D. G.: Morphostructure, tectono-sedimentary evolution and seismic potential of the Horseshoe Fault, SW Iberian Margin. Basin Res, 30: 382-400. doi:10.1111/bre.12225, 2018.

Mason, A., Letter to the Reverend Thomas Birch, D. D. Secretary to the Royal Society, relating to an extraordinary agitation of the Sea there, 31st of March 1761, Philosophical Transactions of the Royal Society, vol. 52, page 477-478, 1761.

~~Mallet, Robert and John Wm. Mallet: The Earthquake Catalogue of the British Association, Transactions of the British Association for the Advancement of Science, 1852 to 1858, Reports 3 and 4, Taylor and Francis, London, 800 pp, 1858.~~

Matias, L. M., Cunha, T., Annunziato, A., Baptista, M. A., and Carrilho, F. (2013). Tsunamigenic earthquakes in the Gulf of Cadiz: fault model and recurrence. Natural hazards and earth system sciences, 13(1), 1-13.

Mezcua, J., and Solares, J. M. M.: Sismicidad del área Ibero-mogrebí, I.G.N., nº 203, Madrid, 301 pp, http://www.ign.es/web/resources/sismologia/publicaciones//SismicidaddelAreaIberoMogrebi.pdf, 1983.

Formatted: English (United Kingdom)

Formatted: English (United Kingdom)

Formatted: English (United Kingdom)

Formatted: English (United Kingdom)

Formatted: English (United Kingdom)

Formatted: English (United Kingdom)

Formatted: English (United Kingdom), Not Highlight

Formatted: English (United Kingdom)

Formatted: English (United Kingdom)

Formatted: English (United Kingdom)

Formatted: English (United Kingdom), Not Highlight

Formatted: English (United Kingdom)

Formatted: English (United Kingdom)

Formatted: English (United Kingdom), Not Highlight

Formatted: English (United Kingdom)

Miranda, J. M., Baptista, M. A., and Omira, R.: On the use of Green's summation for tsunami waveform estimation: a case study, Geophysical Journal International, 199(1), 459-464. https://doi.org/10.1093/gji/ggu266, 2014.

Molloy, M.: Philosophical Transactions of the Royal Society, Vol. 52, Page 142-143, 1761.

Moreira, V. S.: Sismicidade histórica de Portugal Continental, Rev. Inst. Nac. Met. e Geofísica, Março, 1984, 3–79, 1984.

~~National Geophysical Data Center / World Data Service (NGDC/WDS): Global Historical Tsunami Database. National Geophysical Data Center, NOAA, https://www.ngdc.noaa.gov/hazard/tsu_db.shtml, doi:10.7289/V5PN93H7, last access: 1 February 2018.~~

Nocquet, J. M., and Calais, E.: Geodetic measurements of crustal deformation in the Western Mediterranean and Europe. Pure and applied geophysics, 161(3), 661-681, 2004.

Oliveira, C. S.: A sismicidade Histórica em Portugal Continental e a Revisão do Catálogo sísmico Nacional, Laboratório Nacional de Engenharia Civil, Proc. 36/1177638, 235, Lisboa, Portugal, 1986.

Omira, R., Baptista, M.A., and Matias, L.: Probabilistic tsunami hazard in the Northeast Atlantic from near-and far-field tectonic sources, Pure and Applied Geophysics 172 (3-4), 901-920, ISSN: 0033-4553 (Print) 1420-9136 (Online), https://doi.org/10.1007/s00024-014-0949-x, 2015.

Ribeiro, A., Mendes-Victor, L., Cabral, J. M. L. C., Matias, L., and Terrinha, P.: The 1755 Lisbon earthquake and the beginning of closure of the Atlantic, European Review, 14(2), 193-205, doi:10.1017/S1062798706000196, 2006.

Rocque, J.: A Plan of the City of Cadiz and the environs with the Harbour, Bay and Soundings at Low Water also a Particular Plan of the Town and Fortifications from the Collection of Capt. Clark and Improved by the late John Rocque, Topographer to his Majesty. Bibliothèque nationale de France, département Cartes et plans, CPL GE DD-2987, 1762.

Rosas, F. M., Duarte, J. C., Terrinha, P., Valadares, V., and Matias, L.: Morphotectonic characterization of major bathymetric lineaments in Gulf of Cadiz (Africa–Iberia plate boundary): insights from analogue modelling experiments, Marine Geology 261 (1-4), 33-47, https://doi.org/10.1016/j.margeo.2008.08.002, 2009.

Sallarès, V., Martínez-Loriente, S., Prada, M., Gràcia, E., Ranero, C. R., Gutscher, M. A., Bartolome, R., Gailler, A., Dañobeitia, J. J., Zitellini, N.: Seismic evidence of exhumed mantle rock basement at the Gorringe Bank and the adjacent Horseshoe and Tagus abyssal plains (SW Iberia). Earth and Planetary Science Letters 365, 120–131, doi:10.1016/j.epsl.2013.01.021, 2013.

Silva, S., Terrinha, P., Matias, L., Duarte, J. C., Roque, C., Ranero, C. R., Geissler, W., H. and Zitellini, N.: Micro-seismicity in the Gulf of Cadiz: Is there a link between micro-seismicity, high magnitude earthquakes and active faults?, Tectonophysics, 717, 226-241, 2017.

Solares, J. M. and Lopez-Arroyo, A.: The great historical 1755 earthquake: Effects and damage in Spain, J. Seismol., 8, 275–294, https://doi.org/10.1023/B:JOSE.0000021365.94606.03, 2004.

Synolakis, C. E., Bernard, E. N., Titov, V. V., Kânoğlu, U., and Gonzalez, F. I.: Validation and verification of tsunami numerical models, In Tsunami Science Four Years after the 2004 Indian Ocean Tsunami 2197-2228, Birkhäuser Basel, doi:10.1007/s00024-004-0427-y, 2008.

Formatted: English (United Kingdom)
Formatted: English (United Kingdom)
Formatted: English (United Kingdom)
Formatted: Font: Not Italic
Formatted: Font: Not Italic
Formatted: English (United Kingdom)
Formatted: English (United Kingdom)
Formatted: English (United Kingdom)
Formatted: Portuguese (Portugal)
Formatted: English (United Kingdom)
Formatted: English (United Kingdom)
Formatted: English (United Kingdom)
Formatted: English (United Kingdom)
Formatted: English (United Kingdom)
Formatted: English (United Kingdom)
Formatted: Font: Not Italic
Formatted: Font: Not Italic
Formatted: English (United Kingdom), Not Highlight
Formatted: English (United Kingdom)

Terrinha, P., Pinheiro, L. M., Henriet, J. P., Matias, L., Ivanov, M. K., Monteiro, J. H., Akhmetzhanov, A., Volkonskaya, A., Cunha, T., Shaskin, P., and Rovere, M.: Tsunamigenic-seismogenic structures, neotectonics, sedimentary processes and slope instability on the southwest Portuguese Margin. Marine Geology, 195(1-4), 55-73, 2003.

Terrinha, P. , Matias, L., Vicente, J., Duarte, J., Luís, J., Pinheiro, L., Lourenço, N., Diez, S. Rosas, F., Magalhães, V., Valadares, V., Zitellini, N., Roque, C., Mendes Víctor, L. and MATESPRO Team.: Morphotectonics and strain partitioning at the Iberia–Africa plate boundary from multibeam and seismic reflection data, Marine Geology, 267, 3-4, 156-174, https://doi.org/10.1016/j.margeo.2009.09.012, 2009.

Torelli, L., Sartori, R., Zitellini, N.: The giant chaotic body in the Atlantic Ocean off Gibraltar: new results from a deep seismic reflection survey. Marine and Petroleum Geology 14 (2), 125–134, doi:10.1016/S0264-8172(96)00060-8, 1997.

UC-IGN: Tsunami inundation maps along the south west Spanish coast, deliverable d7.1 of the 6th European framework programme project TRANSFER. http://www.transferproject.eu/, last access: 1. August 2018, 2009.

Unknown: An Account of the Earthquake at Lisbon, 31st March 1761: In a Letter from thence, dated 2nd April 1761, to Joseph Salvador, Esq. F.R.S. Philos. Trans. Letter XXVI. pp. 141-142, 1761.

United States Naval Observatory (USNO): http://aa.usno.navy.mil/data/docs/MoonPhase.php, last access: 1 February 2018, 2017.

Wells, D. L. and Coppersmith, K. J.: New empirical relationships among magnitude, rupture length, rupture width, rupture area, and surface displacement, Bulletin of the seismological Society of America, 84(4), 974-1002, 1994.

Wronna, M., Omira, R., and Baptista, M. A.: Deterministic approach for multiple-source tsunami hazard assessment for Sines, Portugal, Nat. Hazards Earth Syst. Sci., 15, 2557-2568, https://doi.org/10.5194/nhess-15-2557-2015, 2015.

Wronna, M., Baptista, M. A., and Götz, J.: On the construction and use of a Paleo-DEM to reproduce tsunami inundation in a historical urban environment–the case of the 1755 Lisbon tsunami in Cascais. Geomatics, Natural Hazards and Risk, 8(2), 841-862, https://doi.org/10.1080/19475705.2016.1271832, 2017.

Zitellini, N., Chierici, F., Sartori, R., and Torelli, L.: The tectonic source of the 1755 Lisbon earthquake and tsunami, Annals of Geophysics, 42(1), http://dx.doi.org/10.4401/ag-3699, 1999.

Zitellini, N., Mendes, L. A., Cordoba, D., Dañobeitia, J.J., Nicolich, R., Pellis, G., Ribeiro, A., Sartori, R., Torelli, L., Bartolome, R., Bortoluzzi, G., Calafato, A., Carrilho, F., Casoni, L., Chierici, F., Corela, C., Correggiari, A., Vedova, B. Della, Gracia, E., Jornet, P., Landuzzi, M., Ligi, M., Magagnoli, A., Marozzi, G., Matias, L., Penitenti, D., Rodriguez, P., Rovere, M., Terrinha, P., Vigliotti, L., and Ruiz, A. Zahinos:.Source of 1755 Lisbon earthquake and tsunami investigated. Eos, Transactions American Geophysical Union,82(26), 285-291, doi:10.1029/EO082i026p00285-01, 2001.

Zitellini, N., Rovere, M., Terrinha, P., Chierici, F., Matias, L. and BIGSETS Team: Neogene through Quaternary tectonic reactivation of SW Iberian Passive Margin. Pure Applied Geophysics, 161, 565–587, 2004.

Zitellini, N., Gràcia, E., Matias, L., Terrinha, P., Abreu, M. A. DeAlteriis, G., Henriet, J.P., Dañobeitia, J.J., Masson, D.G., Mulder, T., Ramella, R., Somoza, L., and Diez, S.: The quest for the Africa–Eurasia plate boundary west of the Strait of Gibraltar, Earth and Planetary Science Letters, 280, 1-4, 13-50, https://doi.org/10.1016/j.epsl.2008.12.005, 2009.